Research Article

Assessing the impact of nutrient loads on eutrophication in the semi-enclosed Izmir Bay combining observations and coupled hydrodynamic-ecosystem modelling

Ozge YELEKCİ[1,3], Valeria IBELLO[1], Bettina A. FACH[1], Filiz KUCUKSEZGIN[2], Caglar YUMRUKTEPE[1,4], Erdem SAYIN[2], Baris SALIHOGLU[1] and Suleyman TUGRUL[1]

[1] Institute of Marine Sciences, Middle East Technical University, Erdemli, Turkey
[2] Dokuz Eylül University, Institute of Marine Sciences and Technology, Izmir, Turkey
[3] CNRS, Laboratoire d'Océanographie et du Climat Expérimentation Et Approche Numériques (LOCEAN), Université Pierre et Marie Curie, Paris, France
[4] Nansen Environmental and Remote Sensing Centre, Bergen, Norway

Corresponding author: bfach@ims.metu.edu.tr

Contributing Editor: Stelios SOMARAKIS

Abstract

Intense human activities may strongly affect coastal environments threatening natural, societal and economic resources. In order to propose adequate measures to preserve coastal marine areas, a thorough understanding of their physical and biogeochemical features is required. This study focuses on one such coastal area, Izmir Bay located in the Eastern Mediterranean Sea. Izmir Bay is a highly populated area subject to many human induced stressors such as pollution and eutrophication, which has been suffering high nutrient loads for decades. Despite the construction of the Çiğli waste water treatment plant in 2000-2001 to reduce eutrophication, such pressures continue to occur. To study the current physical and biogeochemical dynamics of Izmir Bay and their spatial and temporal variability, a three-dimensional coupled hydrodynamic-ecosystem model (Delft3D modelling suite's FLOW and ECO modules) is implemented. Using the model, the effect of excessive inorganic nutrient loading on the marine ecosystem as the main cause of this eutrophication is explored in an effort to advise on mitigation efforts for the Bay focusing on eliminating eutrophication.

Results of different model scenarios show that the Inner and Middle Bay are nitrogen-limited while the Outer Bay is phosphorus-limited. Inner regions are more sensitive to variations in inorganic nitrogen input due to the low (<16) N/P ratio of nutrients in seawater. An increase in inorganic nitrogen triggers eutrophication events with primary production as an immediate response. Conversely, the Outer Bay ecosystem with N/P ratios above 16 is more sensitive to phosphate inputs, of which an increase causes a considerable enhancement in algal production. This study shows the vulnerability of Izmir Bay to anthropogenic nutrient input and model simulations indicate that management plans should consider reducing DIN discharges both in the inner-middle zones of Izmir Bay as well as inputs from the Gediz River. Additionally, phosphate inputs should be reduced to avoid an overall increase of algal production in the Outer Bay, the larger part of Izmir Bay.

Keywords: Eutrophication; semi-enclosed bay; nutrient dynamics; 3-D ecosystem modeling; circulation dynamics.

Introduction

Much of the world population lives in coastal areas and there is an ongoing trend of coastal migration (Small & Nicholls, 2003; Balk *et al.,* 2009). In Europe, more than 50% of the population lives within 50km of the sea (Collet & Engelbert, 2013). This means that coastlines are undergoing large socio-economic and environmental changes, which are expected to continue in the future (Neumann *et al.*, 2015). Therefore, understanding the dynamics of coastal ecosystems is crucial for the efficient management of marine resources, such as fisheries, tourism, and biodiversity.

Izmir Bay (Aegean Sea, Eastern Mediterranean) is a highly impacted coastal region located in the Izmir province of Turkey. With over 4 million inhabitants, it is one of the most populated provinces in Turkey. The area has great economical relevance for Turkey, being the third largest as well as one of the oldest commercial ports in the country. In recent decades, rapid, uncontrolled land development around the region has caused widespread environmental deterioration of the inner zones of Izmir Bay and has threatened the larger region of the Bay (IMST, 1999; Kucuksezgin, 2011; Yucel-Gier *et al.,* 2011). Izmir

Bay receives substantial chemical inputs both from natural (rainfall 15%) and anthropogenic (urban waste water 50%, agricultural activity 10%), and other sources (25%) (UNEP/MAP, 1994) resulting in pollution and eutrophication events. In addition to the large nutrient and organic matter inputs (IMST, 1999; Sayin, 2003; Kucuksezgin *et al.*, 2006), the elongated topography and bathymetry of the semi-enclosed Izmir Bay play an important role in the accumulation of pollutants. The three regions of the bay: Inner, Middle and Outer, are characterized by a restricted circulation across the entire bay and the limited renewal of waters due to the presence of three sills separating the Aegean Sea and Outer III Izmir Bay (70m depth), the Outer II and Outer I bay (Mordogan Strait, 14 m depth) and the Inner and Middle Bay (Yenikale Strait, 13 m depth) (Fig. 1).

As early as the 1950s, red-tide and fish mortality events have been reported (Acara & Nalbantoglu, 1960; Numann, 1995). From the 1980s to the 1990s, eutrophication started to become a major problem with more frequent and severe red tides and anoxic conditions in the bottom waters of Inner Bay, due to discharges of untreated waste waters into the bay (Koray *et al.*, 1996; Bizsel *et al.*, 2001; Gencay & Buyukisik, 2004; Sunlu *et al.*, 2005). High concentrations of dissolved and particulate organic matter, macronutrients (NO_3^-, NH_4^+, PO_4^{3-}) have been observed in both the water column (Bizsel & Uslu, 2000; Bizsel *et al.*, 2009; Yucel-Gier *et al.*, 2011; Kucuksezgin, 2011; Sunlu *et al.*, 2012a; Kukrer & Buyukisik, 2013) and sediments of the Inner Bay (Sunlu *et al.*, 2008; Ozkan *et al.*, 2008; Kontas *et al.*, 2004). In early 2000, the Çiğli Waste Water Treatment Plant (WWTP) was installed as part of the Great Channel Project of Izmir to remove Phosphorus (P), Nitrogen (N) and reactive organic matter in urban waste waters (http://www.izsu.gov.tr). A study carried out soon after the WWTP became operative did not detect any noticeable reduction in N and P concentrations of Inner Bay surface waters (Kontas *et al.*, 2004).

Today, Izmir Bay still displays very high levels of pollution (TARAL-SINHA, 2011; Kucuksezgin, 2011). It has been observed that the bay is characterized by an increasing gradient in nutrient concentration from Outer towards Inner Bay regions, which determines an analogous gradient in primary production (Gencay & Buyukisik, 2004; Kucuksezgin *et al.*, 2005; Yucel-Gier *et al.*, 2011; Sunlu *et al.*, 2012b). Discontinuity of the physical-biogeochemical patterns have been reported to be associated with the local water discharge inputs, especially through the Gediz River (Bizsel *et al.*, 2011).

In terms of physical dynamics, the Outer Bay is characterized by seasonal features of the Eastern Mediterranean, such as water temperatures between ~15°C in winter and 28°C in summer and high salinity between 39 and 40 psu. The Inner Bay region, located on the other side, displays typical features of shallow coastal environments, such as pronounced seasonal variations of physical-chemical parameters, particularly temperature and nutrient concentrations, and absence of vertical stratification (Sayin, 2003; Sayin *et al.*, 2006; Kucuksezgin *et al.*, 2006; Kucuksezgin, 2011). Since the Outer Bay benefits from water exchange with the Aegean Sea, past eutrophication events were reported mainly for the Inner-Middle Bay, in close proximity to the main sources of nutrient loads. Those sources are the waste water treatment plant
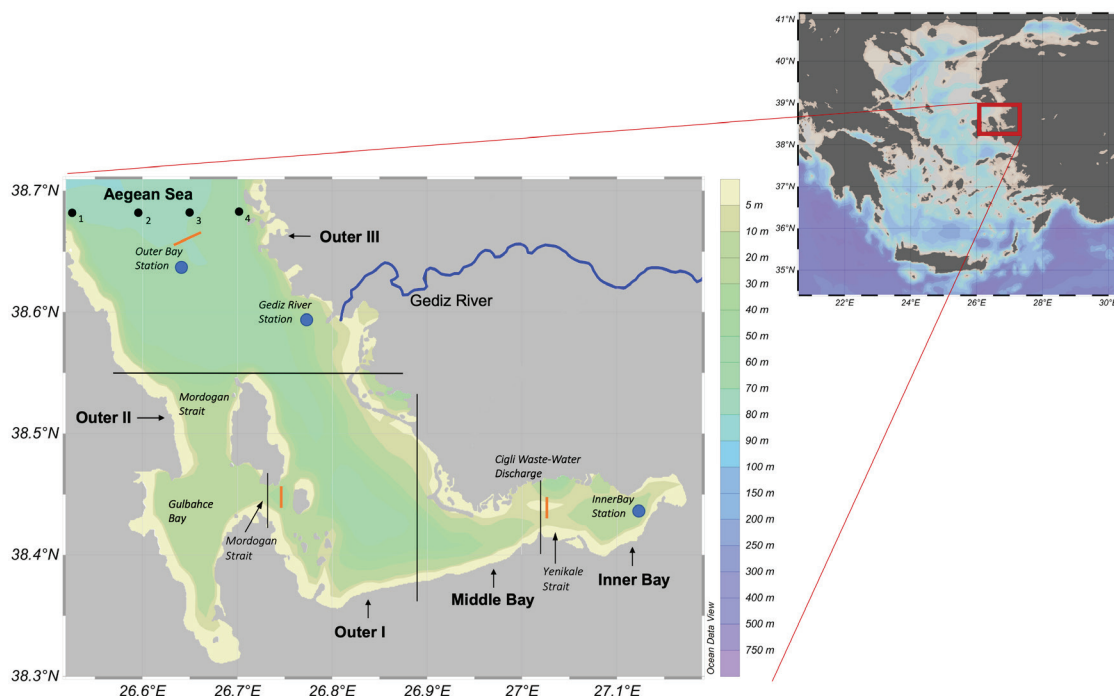

Fig. 1: Location of the study area in the Mediterranean Sea and geography of Izmir Bay. Blue dots mark the location of three stations where measurements were obtained. Black dots mark the four station locations from where in situ nutrient data was used as inputs to the model at the model boundary. The different regions of the bay are delineated by thin black lines. Orange lines denote the three sills present in the Outer and Inner Bay regions.

(Kucuksezgin *et al.*, 2006; Kucuksezgin *et al.*, 2011) and the Gediz river inflow area where agricultural as well as domestic discharges are combined (Kontas *et al.*, 2004; Kucuksezgin *et al.*, 2006; Kucuksezgin *et al.*, 2011).

Although there are observational and, to a limited degree, modelling studies of Izmir Bay (e.g. Ivanov *et al.*, 1997; Sayin, 2003; Sayin & Eronat, 2018; Buyukisik *et al.*, 1997), an in-depth physical and biological assessment of the Bay is still missing. To our knowledge, the current study is the first presenting a three-dimensional coupled hydrodynamic-biogeochemical model for Izmir Bay, with a capacity to test different management scenarios. Previously, a circulation model has been developed by Ivanov *et al.* (1997) to reproduce the circulation of the Bay and later by Sayin (2003) and Sayin & Eronat (2018). A 1-D model used by Buyukisik *et al.* (1997) describes the biogeochemical dynamics of the Bay in a 1-D model only, preventing any resolution of spatial variability.

Lack of basic knowledge can severely impact the efficiency of mitigation actions and strategies implemented at coastal management level. Previous to this study, little has been known about: i) water exchange between the semi-enclosed Izmir Bay and the Aegean Sea, ii) the general water circulation pattern in Izmir Bay, iii) factors controlling primary production/eutrophication/hypoxia in different areas of the bay, iv) the combined effects of different nutrients on the marine ecosystem, over large spatial and temporal scales, or v) the impact of selective increase/decrease of nutrient loads. Resolving these issues is essential in order to estimate the renewal time of water, manage/track pollutant dispersal, and identify those areas particularly vulnerable to anthropogenic pressure.

In this study the current physical and biogeochemical dynamics of Izmir Bay and their spatial and temporal variability are investigated. For this purpose, a combination of observations and model simulations for the years 2008-2010 have been used. The main aim of this study is to explore the effects of inorganic nutrient loads on the marine ecosystem via modelling in an effort to advise on mitigation efforts which focus on eliminating eutrophication in Izmir Bay.

Materials and Methods

In this study, a 3-D coupled hydrodynamic-biochemical model, originally developed by Delft University of Technology (Roelvink & Van Banning, 1994; Lesser, 2004) for coastal and estuarine ecosystems, is implemented to investigate the nutrient dynamics of Izmir Bay. The framework of the DELFT Model Package consists of several modules that can interact (https://www.deltares.nl/en/software-solutions/). In this study, the modules Delft3D-FLOW and Delft3D-Eco are used as described in detail below. In addition, physical and biochemical in-situ data collected in the Bay is used to validate model results.

Field Measurements

Physical and chemical data from Izmir Bay were collected during eight seasonal cruises undertaken from March 2007 to July 2010 within the framework of the TARAL-SINHA project. The station network for physical and biogeochemical measurements covered the entire Izmir Bay area (see Fig. 3 for station locations). At all stations (n=31) continuous temperature and salinity measurements were carried out in the water column with a CTD. Biogeochemical parameters were measured at standard depths (0m, 5m, 10m, 15m, 20m, 30m, 40m, 50m, 60m, bottom) over a subset of 15 stations.

Hydrodynamic Model

Delft3D-FLOW is a multi-dimensional hydrodynamic simulation program that computes non-steady flow and transport resulting from tidal and meteorological forcing (Delft Hydraulics, 2009). It solves 3D non-linear shallow water equations, derived from the 3D Navier Stokes equations for incompressible free surface flow, under the Boussinesq approximation. The system of equations consists of the horizontal equations of motion, the continuity equation, and the transport equations for conservative constituents. Vertical velocities are computed from the continuity equation.

The Izmir Bay model grid is set to 0.5 x 0.5 km horizontal and 20 layer vertical resolution extending into the Aegean Sea to 38.75 N. There are two open boundaries located north and west where the model connects Izmir Bay with the Aegean Sea. The flow boundary conditions are set as the Riemann type boundary condition with Riemann invariant equivalent to 0 m s^{-1}. This ensures an open boundary to the Aegean Sea, where the inflow and outflow at the boundary are not forced, but is determined by the model in response to the data collected at the Outer Bay stations (see Fig. 1, stations 1-4). Heat and salt transport boundary conditions are defined as time and space dependent using *in situ* measurements vertically interpolated to sigma layers. Information on the data set used is given above.

The model was initialized in March 2007 calibrated with uniform temperature and salinity water column values in accordance with *in situ* measurements for the month of March (15°C, 39.1‰), when the water column is well mixed. The Cross-Calibrated Multi-Platform Wind Vector Analyses (CCMP) product of remotely sensed wind stress level 2.5 data provided by the NASA Jet Propulsion Laboratory (ftp://podaac-ftp.jpl.nasa.gov/allData/ccmp/L2.5/flk/) was applied to construct wind forcing. Atmospheric forcing input in the form of air temperature, relative humidity, and cloudiness was obtained from the European Centre for Medium-Range Weather Forecasts (ECMWF) ERA-Interim data set (http://apps.ecmwf.int/datasets/data/interim-full-daily/levtype=sfc/) and applied spatially uniform, since variation over this small domain can be ignored.

Fresh water inputs (annual influxes) were obtained

Medit. Mar. Sci., 22/3 2021, 677-696

679

from the Mediterranean Pollution Monitoring and Research Programme (MED POL) reports (IMST-167, 2007; IMST-180, 2008). Seasonally fluctuating monthly fresh water discharge levels were then constructed by using precipitation data retrieved from the ECMWF ERA-Interim data set, as no monthly data on fresh water was available for the time frame of this study. Since no data is available on water input through the WWTP or for rain drainage in the Inner Bay, water input for the model was estimated as follows: To represent the fresh water contribution of Çiğli Waste Water Treatment Plant a point source was added in the vicinity of its location in the Inner Bay. To mimic the rain drainage along the shallow inshore regions, five point sources of fresh water were added along the Inner Bay and five along Outer II Bay, specifically at Gulbahce Bay (Fig. 1). A fraction of the calculated monthly Gediz River flux (5% for each point) is prescribed at these points into the Bay.

Ecosystem Model

The ecosystem model Delft3D-ECO, containing the sophisticated algae model BLOOM (Blauw *et al.*, 2009; Los, 2009), is off-line coupled to the hydrodynamics model (Fig. 2). The BLOOM algal model distributes available resources optimally among different types of algae thereby selecting the best adopted combination of phytoplankton types at each time step and location (Los, 2009). In the model setup for Izmir Bay, three different phytoplankton species, namely autotrophic flagellates, dinoflagellates, and diatoms are defined. These phytoplankton groups in BLOOM are designed to simulate natural competition between functional groups or individual species for potentially limiting resources. To account for variations in internal stoichiometry of a species, three subunits labelled 'types' under each model species, represent the physiological state of each species under different conditions of limitation (nitrate; phosphate; light). Thus, functional groups are able to become dominant either due to a high growth rates or low resource requirement. Through this feature, the selection of species depending on their adaptation to limiting factors and competition is effectively modeled.

In addition, nutrient fluxes, dissolved oxygen and organic matter concentrations across the sediment-water interface are simulated with the sub-model SWITCH (Sediment Water Interaction by Transport and Chemistry) using mass-balance equations (Delft Hydraulics, 2009). This sub-model consists of three layers (aerobic, oxidized, anaerobic), situated between the seawater interface and the inactive layer at the base of the sediments. The progressive decrease of dissolved oxygen in these layers represents oxygen consumption through degradation of detritus and for nitrification and chemical oxidation in the aerobic layer. The amount of detritus settling
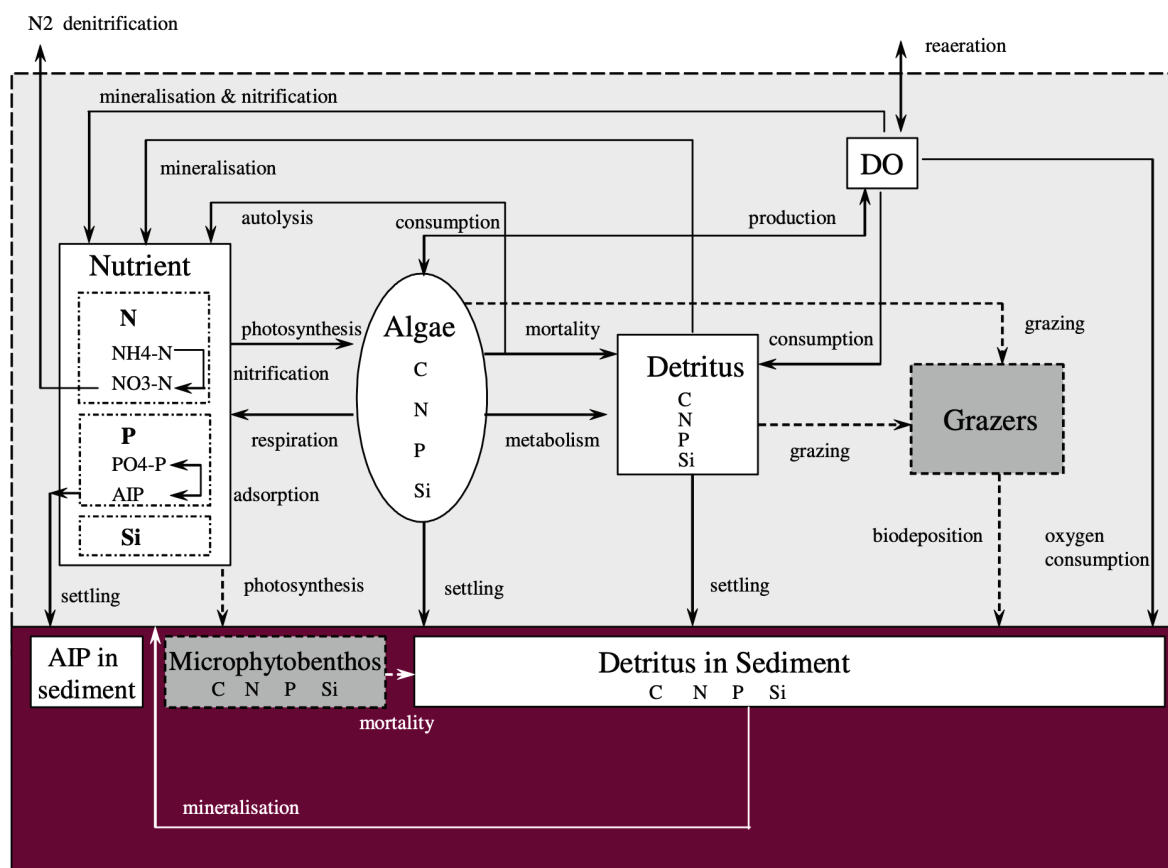

Fig. 2: Overview of compartments of the ecosystem model BLOOM used (adapted from Blauw *et al.*, 2009). The model adapted to Izmir Bay does not include the state variables marked in dark grey (Grazers and Microphytobenthos) or processes marked with dashed lines.

to the sediment is computed by Delft3D-ECO and used by SWITCH as input. Detritus is subject to settling, resuspension, incorporation from the boundary layer into the sediment, degradation, and burial. Ammonia (NH_4), produced during the degradation of detritus, can be transported vertically and converted through nitrification to NO_3 under aerobic conditions. Nitrate (NO_3), produced through nitrification, can be transported vertically and is subject to denitrification below the aerobic layer. Phosphate (PO_4) is similarly produced during the degradation of detritus and can be transported vertically. Local production of detritus by benthic phytoplankton is not considered.

The ecosystem model is run on the same three-dimensional spatial grid and time step as the hydrodynamic model. Current velocity, temperature, and salinity fields for the hydrodynamic model time step (12 hours) were used as input variables for the ecosystem model. As for the hydrodynamic model, the ecosystem model was initialized in March 2007 with uniform nutrient concentration values from the available measurements (see below) for the month of March, when the water column is mixed and nutrient concentration is uniform. The ecosystem model underwent a spin-up period of ten months followed by a running period of three years from January 2008 until January 2011. Sources of nutrient loads prescribed in the model are fresh water discharges, atmospheric input, and input through the open boundary. For the open boundaries, nutrient inputs were obtained from the dataset (see below) from stations 1-4 at the Outer III Bay (Fig. 1). Atmospheric deposition fluxes were obtained from estimations for the northern Levantine basin (Kocak *et al.*, 2010). Gediz river nutrient and dissolved oxygen concentrations were obtained from MED POL reports (IMST-167, 2007; IMST-180, 2008). Due to a lack of data on monthly nutrient discharge for Gediz river, annual nutrient and dissolved oxygen concentrations were obtained from MED POL reports (IMST-167, 2007; IMST-180, 2008). Using monthly precipitation data, monthly nutrient and dissolved oxygen concentrations were calculated from the annual data by scaling the annual inflow relative to the monthly precipitation data in order to reproduce a realistic estimate of seasonality in nutrient fluxes.

Since no nutrient measurements were available for rain drainage points, data measured in similar regions were adapted. For Gülbahce Bay region (Outer Bay II), PO_4^{3-} (hereafter called PO_4) values obtained by the MED POL project (IMST-167, 2007; IMST-180, 2008) for Lamas River (Mersin, Turkey) were used, for the Inner Bay region, PO_4 values were used from the TARAL-SINHA project at the Çiğli WWTP (TARAL-SINHA, 2011). NO_3 and NH_4 inputs were then tuned with respect to distribution of the N/P ratio for each region of the Bay, computed from the available nutrient measurements. The resulting nutrient inflow estimation was in agreement with the N/P ratio of between 9.8 and 10.4 as reported in the 2010 report of Çiğli WWTP, recently made available (Yili Faaliyet Raporu, 2010).

Levels of organic material carried by Gediz river and rain drainage, and via Cigli WWTP were computed from the BOD_5 (5-day biological oxygen demand)

measured at Gediz river and Çiğli WWTP respectively, using empirical relations as an approximation due to the lack of direct measurements. The following relationships of reactive $DOC=BOD_5/3$ for rivers and rain drainage, reactive $DOC= BOD_5/2.5$ for waste waters, reactive $DON=DOC/10$, $DOP=DOC/200$, $DOSi=DOC/200$ are assumed. Particulate C, N, P, and Si values were set to the dissolved values (Tugrul personal communication) as initial conditions to emulate the correct nutrient budget. Following the spin-up period of 10 months, the model was observed to have balanced dissolved/particulate forms.

Simulations

The reference model simulation with the coupled hydrodynamic-biochemical model was run for three years (2008-2010). After a ten-month spin-up period (March to December 2007) the model was run continuously for three years until January 2011.

Following validation of the model, a set of experimental ecosystem model scenarios were designed (Table 1) to evaluate the ecosystem response to possible future changes in terms of inorganic bioavailable forms of nutrients (+/- 10% of current inputs). Five different combinations of DIN and PO_4 loads were tested. The hypothesis tested in these scenarios were: *i*) No improvement in PO_4 treatment methods, thereby levels remain unchanged (simulations A and B) or levels increase (simulations C, D, and E), *ii*) Treatment of DIN is improved, so a reduction occurs in DIN loads (simulations B and E), and *iii*) No improvement in DIN treatment methods thereby levels remain unchanged (simulation C) or DIN levels increase (simulations A and D). As urbanization increases, the load of PO_4, a pollutant of domestic origin, increases. As reported by Kontas *et al.* (2004), Kucuksezgin *et al.* (2006) and Sunlu *et al.* (2012a,b) after the treatment facility was constructed, PO_4 concentrations in the WWTP effluent increased. Therefore, to reproduce real life scenarios, a reduction in PO_4 levels was not considered. Increases and decreases in PO_4 levels and DIN loads were tested separately in order to evaluate the different responses of the contrasting N-limited and P-limited environments.

Table 1. List of scenario simulations.

Simulation	PO4	DIN
Reference	-	-
A	-	+10%
B	-	-10%
C	+10%	-
D	+10%	+10%
E	+10%	-10%

Medit. Mar. Sci., 22/3 2021, 677-696

681

Model validation and skill assessment

Both the hydrodynamic and ecosystem model results were validated using data obtained for Izmir Bay water column between 2008-2010 collected within the framework of the TARAL-SINHA project (see section 2.1). Although the figures and discussion in this study focus on one calendar year (2009), a statistical analysis using all available data is provided to achieve a robust model validation.

Specifically, three statistical measures, commonly used to assess model skill of coupled marine ecosystem models (Stow *et al.*, 2009) are calculated: the correlation coefficient (*r*), the root mean square error (*RMSE*), and average absolute error (AAE). The definitions of chosen parameters are given by:
r, the correlation coefficient of model results (P) and observations (O):

$$r = \frac{\sum_{i=1}^{n}(O_i - \bar{O})(P_i - \bar{P})}{\sqrt{\sum_{i=1}^{n}(O_i - \bar{O})^2 \sum_{i=1}^{n}(P_i - \bar{P})^2}}$$

RMSE, root mean squared error:

$$RMSE = \sqrt{\frac{\sum_{i=1}^{n}(P_i - O_i)^2}{n}}$$

AAE, average absolute error:

$$AAE = \frac{\sum_{i=1}^{n}|P_i - O_i|}{n}$$

The correlation coefficient, *r*, varies between -1 and 1, negative values indicating negative correlation. Values close to -1 indicate an inverse correlation, while values close to 1 indicate a direct correlation. Values close to 0 indicate very poor correlation. Although r indicates performance of a model compared to an observational data set, it does not measure the actual difference between model and observational results. RMSE and AAE, on the other hand, are direct measurements of error between observations and model computed values. AAE is the simple average of the absolute difference between model results and observations, while RMSE is the square root of the mean square error which provides more weight to the largest errors. Values of RMSE and AAE close to 0 denote good model performance.

Model misfit, defined as the difference between observations and model results, versus observations are also used to address the shortcomings of the reference model simulation. Plots are color-coded with respect to time and space. This representation clearly reveals weaknesses and strengths of the model, highlighting the density of error points in certain ranges of observation values.

Results

Hydrodynamic Model Results

Outer Bays

Surface circulation of Izmir Bay illustrates that Aegean Sea water enters the Bay from the north during 2009. It follows the western coastline while outflow from the Bay follows the eastern coastline creating a cyclonic gyre in Outer III (Fig. 3A-D). The gyre varies in strength between seasons. This flow pattern only changes during summer (Fig. 3C), when there is a strong inflow along the eastern coast of the Bay and the Gediz River plume is more noticeable. The river plume moves southward into and through Outer I, independently of the general circulation of Outer III. The remnants of the river plume sporadically enter Middle Bay. Along the western coastline, the branch of inflowing Aegean Sea water enters Outer II Bay, passes Mordogan Strait, turns east, and reaches Outer I Bay. In Outer I Bay, a wide southward surface current is observed for the winter seasons (at the beginning and end of 2009), which evolves into an anticyclonic gyre in the summer season, that has also been reported as Middle Gyre by Sayin (2003), Sayin & Eronat (2018) and Ivanov (1997, 1998). Dominant winds are westerly during summer.

The simulated temperature and salinity distributions for the Outer Bay regions overall are in good agreement with observations (overlaid as colored circles in Fig. 3) except for a few local exceptions. In winter, warm water from the Aegean Sea enters the bay from the north and occupies the Outer III region. Towards the Inner Bay, temperature gradually decreases forming a horizontal gradient due to more rapid cooling of the shallow water column in the Inner Bay compared to deeper waters. Salinity of 39.0 psu in the Outer III region reflects the Aegean Sea influence, which decreases to ~38.0 psu at the Gediz River mouth. In spring, Aegean Sea waters occupy the northeast while towards the inner regions, at the Gediz River mouth and southward, the surface salinity decreases to 35.0 psu. The river inflow influences the Outer I Bay, while local freshwater discharges impact the salinity of the Outer II Bay.

In summer, Aegean Sea waters measuring ~21°C occupy the Outer Bay while surface waters increase remarkably (~28°C) towards the shallow Inner Bay (Fig. 3G), demonstrating that inflowing cooler waters followed the eastern coastline of the Outer III and Outer I Bays, lowering temperatures in these areas, which is not apparent from observations. Simulated surface salinity values match observations, showing the dominance of Aegean Sea waters. In summer, the Gediz River dries up and no fresh water influence is seen in the Outer III or Outer I regions of Izmir Bay. In autumn, winds increase resulting in mixing and cooling of the surface layer, decreasing surface temperatures to ~19°C within the Bay (Fig. 3H)

At Outer Bay station (see Fig. 1 for station location at 60m depth), the time-depth distribution illustrates the development of a seasonal thermocline and halocline fea-
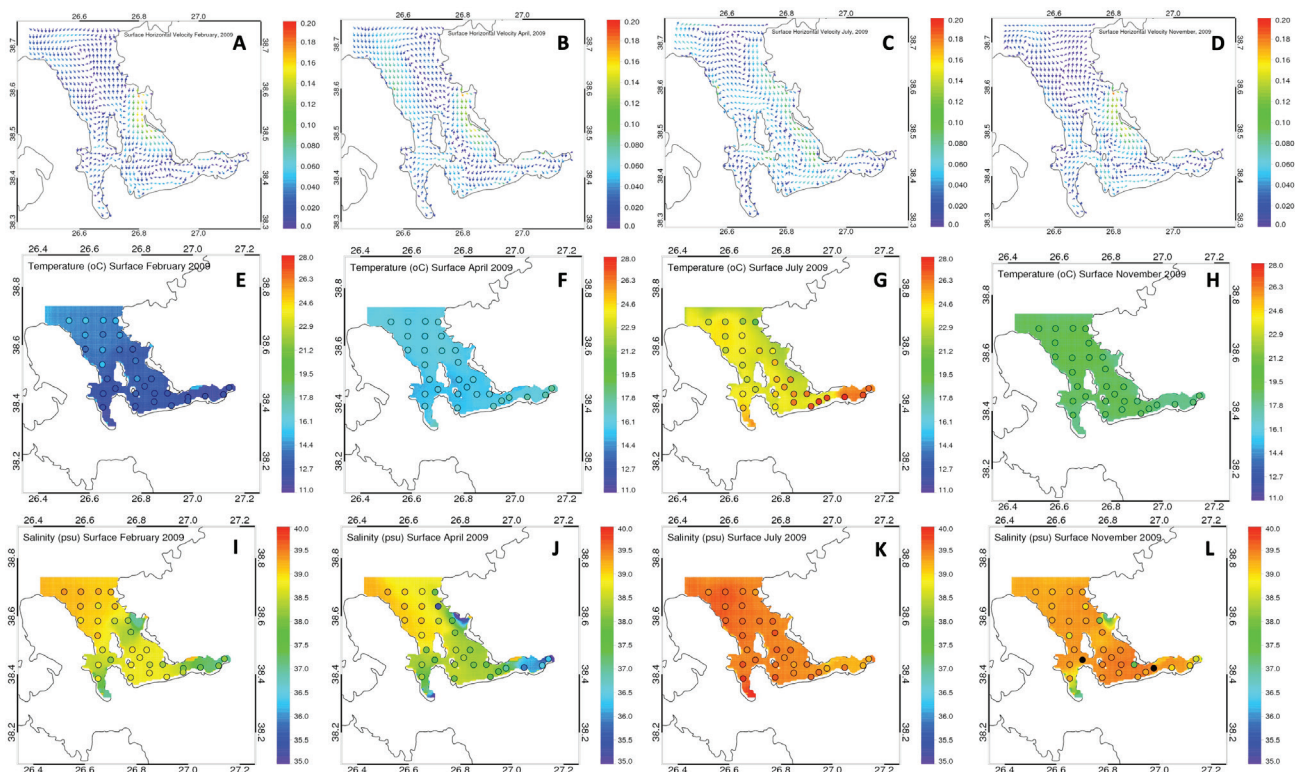
682

Medit. Mar. Sci., 22/3 2021, 677-696

Fig. 3: Simulated surface current velocities in m/s (1st row), and sea surface temperature in °C (2nd row), and surface salinity in psu (3rd row) for February (1st column), April (2nd column), July (3rd column), and November (last column) 2009. Model simulated surface temperature and salinity are plotted with in-situ measurements overlaid in colored dots. Black dots mark missing data.

tures in the surface layer (Fig. 4B, D). In winter however, the water column is entirely mixed with simulated temperature and salinity values homogeneous, reaching 14-15°C and 39.0-39.2 psu, respectively. In the simulations, this trend is interrupted when surface salinity decreases to ~38.5 psu, not confirmed by observations. With the onset of warming in late spring, a thermo/halocline develops within the Outer Bay. A surface layer of 15m depth increases in temperature to 20-21°C in spring and salinity reaches 39.2-39.4 psu, with occasional fresh water intrusions similar to winter. The water column is strongly stratified during summer with a thermo/halocline depth around 20 m. Upper layers reach 28°C and 40.0 psu, whereas deep waters record lower temperature (17-18°C) and salinity (39.2 psu) in summer, consistent with observations. Starting from early autumn, the onset of the thermo/halocline deepens and in early December, with the start of winter mixing it completely disappears. Comparisons between data sets are not possible for autumn, because of the lack of T and S in situ data at this station.

Middle and Inner Bays

The simulated temperature and salinity distributions for the Middle and Inner Bays are in slightly less good agreement with observations compared to Outer Bays. Simulated surface currents show inflow of water to the Inner Bay from Middle Bay along the northern coast and outflow from the Inner Bay into Middle Bay along

the southern coast (Fig. 3A-D). In the Inner Bay a weak anti-cyclonic pattern exists year-round. In winter, a horizontal gradient with decreasing temperature from warmer Aegean water to the cooler Inner Bay is formed. At the border between the Middle and Inner Bay, a similar horizontal gradient is formed in the salinity field (Fig. 3I) due to increased fresh water flux in winter. Salinity was determined as ~38.0 psu in the Inner Bay. In spring, the shallow regions of the Bay react rapidly to the onset of warming and the simulated horizontal salinity gradient from east (between Inner and Outer III Bay) to west (between Outer I and Outer II Bay) is more pronounced (Fig. 3J) than in winter. In summer, surface waters of the Middle and Inner Bays are remarkably warmer (~28°C) compared to Outer Bays (Fig. 3G) due to warming in the shallow waters. In autumn, an increase in freshwater input is seen again.

The time-depth distributions of in-situ temperature and salinity in the Inner Bay station (see Fig. 1 for station location at 18m depth), show two important features: i) this shallow region of Izmir Bay is vertically mixed in all seasons, and ii) the physical properties of the water column show a pronounced seasonal cycle (Fig. 4A,C colored dots). In winter, lower temperatures of 11-12°C and lower salinities of 36.5-37.0 psu compared to the rest of the Bay are observed. Towards late summer, temperature peaks at 28°C and salinity at 40.0 psu. Model results are in good agreement with the observations.
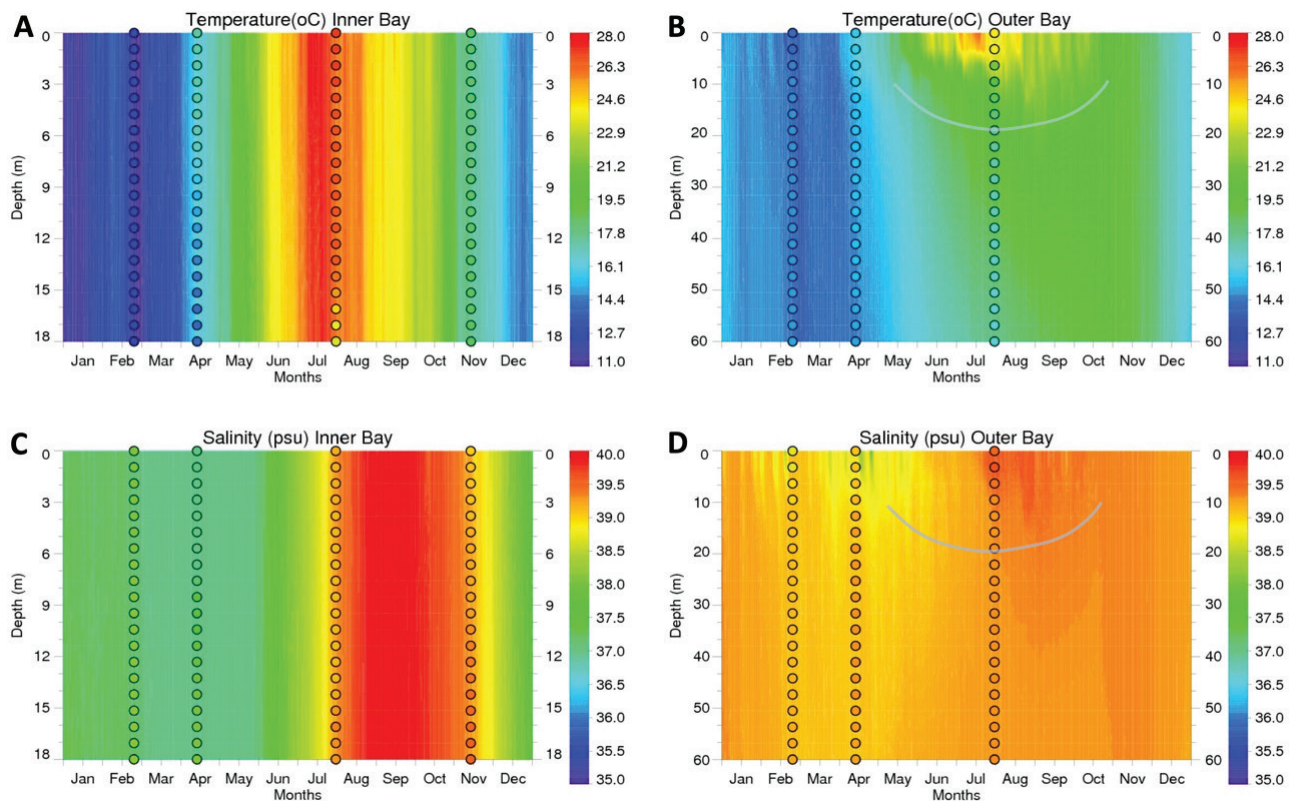
Fig. 4: Simulated time-depth distributions (background) for 2009 in comparison to measurements (colored dots) of temperature in the A) Inner and B) Outer Bays, as well as salinity in the C) Inner and D) Outer Bays. Observations for Autumn 2009 were not available for the Outer Bay. Thin grey lines indicate the approximate location of the seasonal thermocline (B) and halocline (D) in the Outer Bay.

Hydrodynamic Model Validation

Above results show that the modelling system is capable of resolving the temporal and spatial distribution of temperature and salinity of Izmir Bay in 2009. However, it is of importance to assess the overall skill of the model. To do so, model results are compared with the available *in situ* data set of observations collected over a 20-month period (November 2008-July 2010) for the entire water column (Figs 3, 4).

Comparison of the modeled temperature with the ob-

servations (Table 2) shows that the model performs best in autumn and poorest in summer. In winter, correlation coefficients (*r*) are high with values above 0.8 for both years. In 2009, the model displays a reasonable match with observations, but in February 2010 the model generates a poorer fit to observations when estimating the maximum and minimum temperatures. This can also be seen in error statistics (Table 2). The root mean squared error (RMSE) and average absolute error (AAE) are higher in February 2010. Given the high *r* value for this season, this signifies that the model reproduces conditions well,

Table 2. Summary of statistics calculating model skill for temperature and salinity. Negative values of correlation coefficient (r) indicate negative correlation, values close to 0 denote poor correlation, values close to 1 signify good correlation. Values of both root mean squared error (RMSE) and average absolute error (AAE) close to 0 represent good model performance.

	Temperature (ºC)			Salinity (psu)		
	r	RMSE	AAE	r	RMSE	AAE
November 2008	0.64	0.25	0.20	0.55	0.22	0.17
February 2009	0.89	0.72	0.61	0.81	0.23	0.14
April 2009	0.50	0.73	0.64	0.82	0.37	0.28
July 2009	0.86	2.13	1.87	0.35	0.28	0.11
November 2009	0.46	0.33	0.26	0.073	0.80	0.16
February 2010	0.87	0.92	0.77	0.43	0.78	0.28
April 2010	0.73	1.03	0.95	0.73	0.24	0.20
July 2010	0.90	1.77	1.49	0.16	0.68	0.35

684

Medit. Mar. Sci., 22/3 2021, 677-696

but that the overall range of simulated values produce similar bias. In April, the model overestimates the lower temperatures in 2009 and consistently underestimates temperature throughout 2010. Although r values are high in July, indicating a high correlation, the biggest mismatch occurs in this season. The model underestimates the temperature maxima and minima with relatively large errors In November, r values are lower compared to other seasons, but associated with the smallest errors.

Overall, the model fittingly reproduces temperatures for 2008 and 2009 with the exception of underestimating maximum values. The model misfit analyses (Fig. 5) show model performance to be better in transient seasons, spring and specifically autumn and within reasonable limits (+/- 2°C) in winter (Fig. 5A, C). In summer, it does not produce temperatures above 24 ° C or below 18 ° C with errors of up to 4.5°C. This may be because the water column in the model is less stratified than observed. This results in a deeper mixed layer, rendering the model less capable of generating extreme high and low temperatures. Spatially, the majority of high errors occur in the Outer I, Outer III and Middle Bays, whereas, in shallower Inner and Outer II Bays, errors are within the normal range of data variation (Fig. 5B, D).

In terms of salinity, comparison of model results versus measurements (Fig. 5, Table 2) shows that model performance is better in 2009 than in 2010. In February 2009, the model performs better towards maximum observed salinities but underestimates lower salinities. Error margins are within acceptable limits in 2009, but are greater in 2010. For April, r values higher than 0.7 together with reasonably low error margins in both years indicate good correlation. In July, the model shows easonable performance for the majority of lower salinities but displays poor skill in reproducing maximum values observed in this season with large discrepancies. Model

error is greater in July 2010 than for any other season. In November, although r values are on average lower than other seasons, reduced error margins indicate better model performance.

The misfit analyses indicate that model performance is best at salinities around 39 psu (Fig. 5C). Below this value, model misfit increases, especially in winter and spring when the influence of fresh water input was most significant. These mismatches mainly occur in shallow regions of the Inner, Middle and Outer II Bays that are the direct receivers of fresh water from small outlets, and in a few points with very large errors in Outer III Bay, in vicinity of Gediz River plume. This is to be expected as there is no data available on local freshwater inputs to force the model realistically. In summer, the model does not reproduce the observed salinity of over 40 psu for November 2009 and July 2010 (Fig. 5C, D), indicating a systematic underestimation of salinity values that is more pronounced with increasing salinity. The majority of these errors are located at Outer I Bay where coastal salt flats are present and at a few points in Outer III Bay. As shown for temperature, the model underestimates minima and maxima, but performs reasonably at average salinity values.

Ecosystem Model Results

The ecosystem model resolves the time-dependent distribution of biogeochemical properties of Izmir Bay. The Bay is oligotrophic with two very productive areas in the Inner and Middle Bays and in Outer III, influenced by the Gediz river discharge. In order to simplify the outcomes description, results related to Inner and Middle Bays and the Outer Bay have been grouped in two separate sections.
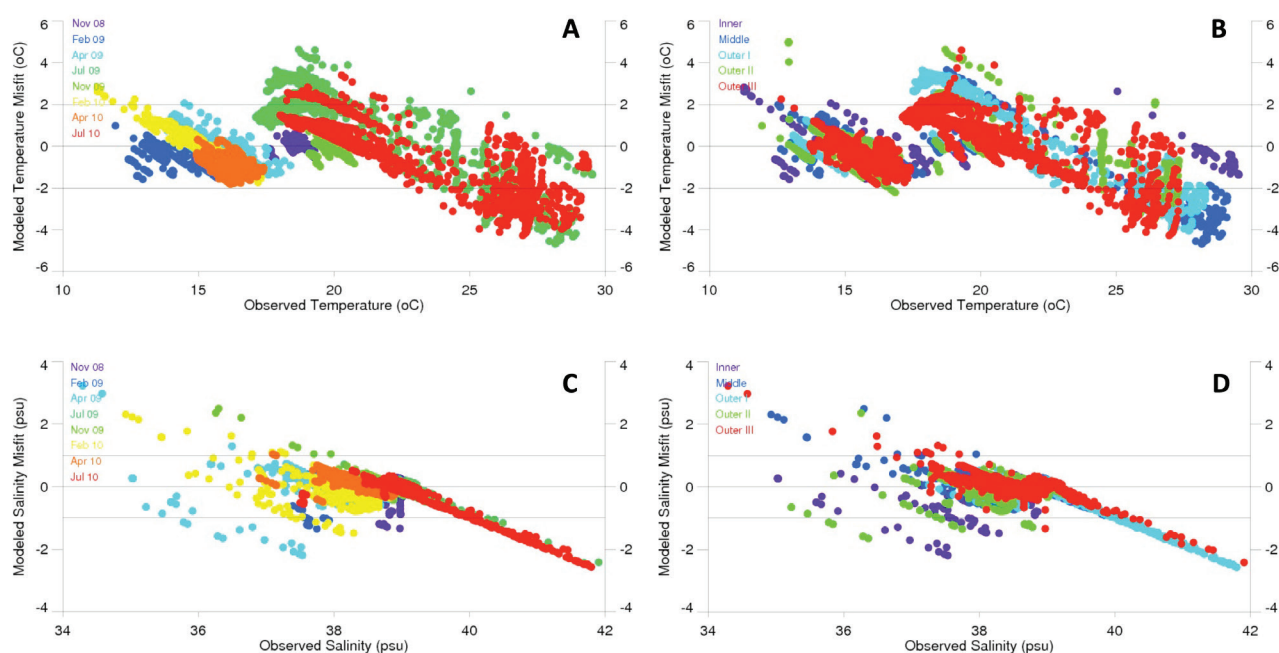

Fig. 5: Measurements of model misfit (model-observations result) versus observations color coded with respect to time for temperature with respect to A) time and B) region, as well as for salinity with respect to C) time and D) region.

Medit. Mar. Sci., 22/3 2021, 677-696

685

Outer Bays

Outer Bay displays much less variability with respect to the inner areas. The area of highest variation is the Gediz river area, where outflow and inorganic/organic inputs is known to vary drastically during the year. The most oligotrophic area is the Outer Bay III.

The model shows moderate levels of chlorophyll concentration in winter (min-max: 0.6 - 3.1 mg m⁻³) and spring (min-max: 0.3 - 3.0 mg m-3) which decrease in summer (0.1-1.1 mg m-3) and slightly increase in autumn (min-max: 0.1 - 5.5mg m-3) mainly in the area influenced by the Gediz river (Fig. 6). Chl-a ranges are generally in good agreement with the observations (min-max ranges in winter: 0.5-3.2; spring: 0.4-4.9; summer: 0.2-2.5; autumn: 0.2-1.6 mg m-3) even though the model slightly underestimated the higher values measured in the inner area of the Outer Bay (Outer I). The model also indicates high production in the immediate proximity of the Gediz river (Fig. 6), which could not be compared with data, as no measurements were collected. Modeled DIN level is quite stable at 0.5 μM for most sea-

sons, in accordance to observations (winter: 0.-0.5; spring: 0.-0.7; summer: 0.1-0.5; autumn: 0.2-1.4 μM). Excessive DIN values are predicted for spring in response to the high nutrient inputs from Gediz River. Model generated values of PO_4 and measurements display both spatial and seasonal variations, ranging between 0.01 and 0.1μM for the Outer Bay in all seasons, in agreement with measurements (Fig. 6). Modeled POC spatial distribution in the innermost Outer Bay is influenced by the Gediz River, displaying maximum values in its immediate vicinity during all seasons except summer. The elevated values are confirmed by the observations but in winter differ from the model values. For the rest of the Outer Bay, except the innermost areas, model results correctly reproduce the observations ranging between 5 and 27μM. The simulated DIN/PO_4 ratios range between 5.3 and 36.4 (ave±sd: 28.8±16.3), indicating P-limitation over the year (Fig. 7). In Gediz River area, the variable loads of DIN, high in winter and spring and limited in summer and autumn, drive a switch between P-limitation (38.5-78.9) to a partial N-limitation (10.4-18.5). Observations in this area, confirm the general pattern of the DIN/PO_4 ratios but with a
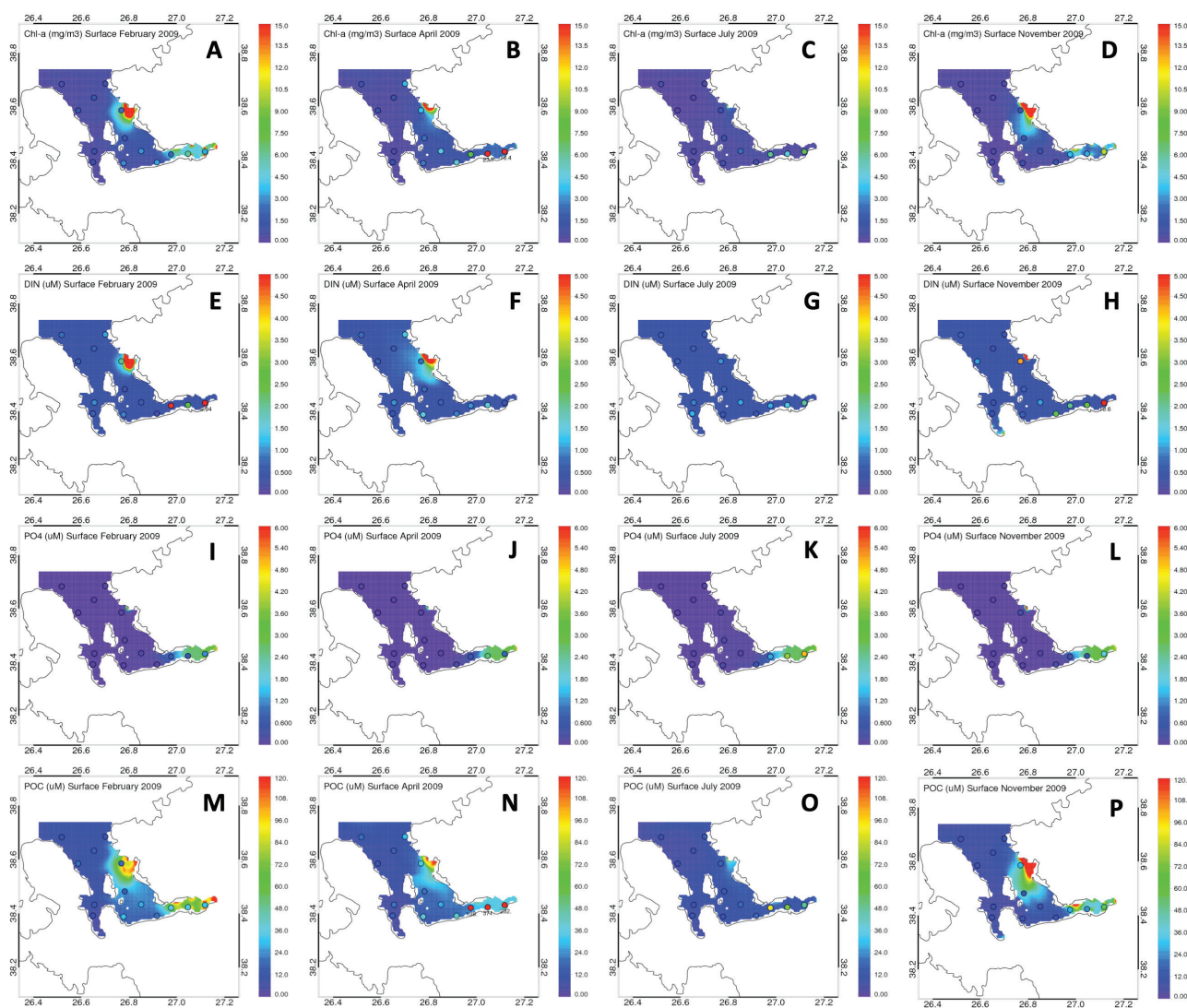

Fig. 6: Surface simulation results (background) for 2009 in comparison to measurements (colored dots) of Chl-a (1ˢᵗ row), DIN (2ⁿᵈ row), PO4 (3ʳᵈ row) and POC (last row) for February (1ˢᵗ column), April (2ⁿᵈ column), July (3ʳᵈ column), and D) November (last column). Values of observations that exceed the color bar ranges are noted next to the station locations.
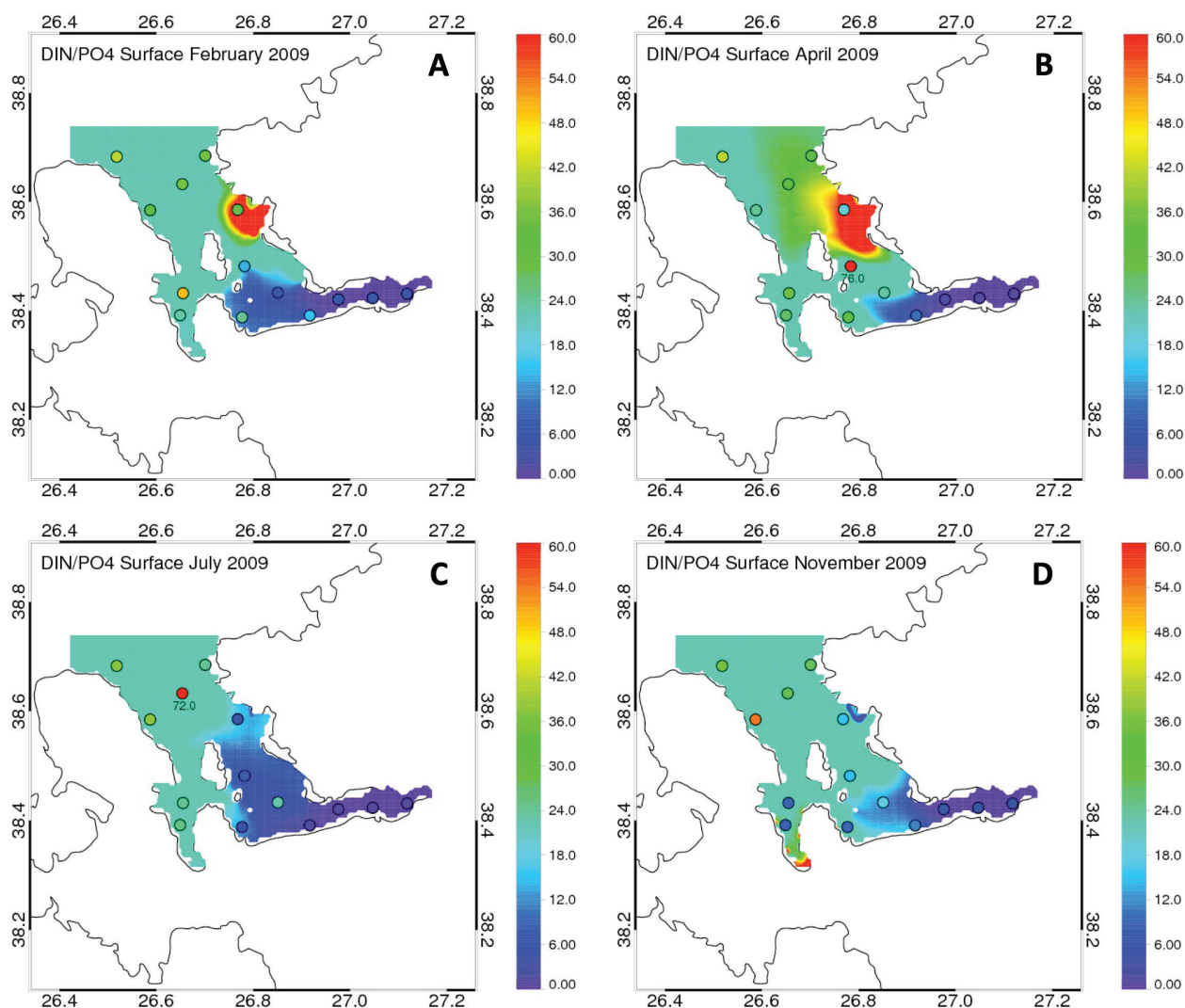
Fig. 7: Surface DIN/PO4 simulation results (background) in comparison to measurements (colored dots) in A) February, B) April, C) July, and D) November 2009.

variable intensity (winter: 28.3, spring: 19.5, summer: 5.70, autumn: 15.14) due to the variations in DIN concentrations, which are not entirely captured by the model (Fig. 7).

The time-depth distributions of modelled Chl-show slightly higher values in the surface layer with respect to depth throughout the year (Fig. 8B). The observed Chl-*a* maximum at ~40-50m in Outer Bay is matched by the model in intensity but located at 10-15m depth. Modelled DIN displays a homogeneous concentration over the entire water column in agreement with the pattern and levels of measurements. In winter the model slightly underestimates DIN concentration (Fig. 8D). A discrepancy in the deeper layers is seen in spring and summer, when modelled DIN slightly overestimates the observed values (Fig. 8D). Modelled PO_4 displays low values throughout the year, in accordance to observations (Fig. 8F). Modeled POC shows a weak variation over the water column, confirmed by measurements (Fig. 8H). However, a higher seasonal variability is seen in the model with respect to the observations. Modeled POC values fit observations best in autumn compared to other seasons.

Inner and Middle Bays

Biogeochemical properties of the Inner and Middle Bays at the surface follow a clear seasonal cycle (Figs 6, 7). The model shows high production in winter and autumn (maximum Chl-*a*: 5.1 mg m^{-3}), confirmed by the observations (1.8- 5.7 mg m^{-3}), followed by a progressive decrease in spring (2.8-3.1 mg m^{-3}) and summer (0.1-1.1 mg m^{-3}), which was not reported in the measurements (spring: 4.9-23.7 mg m^{-3}, summer: 0.7-6.8 mg m^{-3}). Modelled DIN and PO_4 show a different pattern. Whilst during the year, DIN is generally low (0.5-0.7 μM) with respect to observations (0.30-8.54 μM), PO_4 reproduces higher concentrations (1.15-3.05 μM) similar to the measured values (0.62-4.62 μM). The gradient between the Inner Bay and the Outer Bay is well defined, even though seasonality in the model is weaker than for observations. Modelled POC displays maximum POC concentrations in winter (model overestimates measurements), followed by a progressive decrease in spring reaching the minimum in summer (model underestimates measurements). Comparison with measurements show that the main
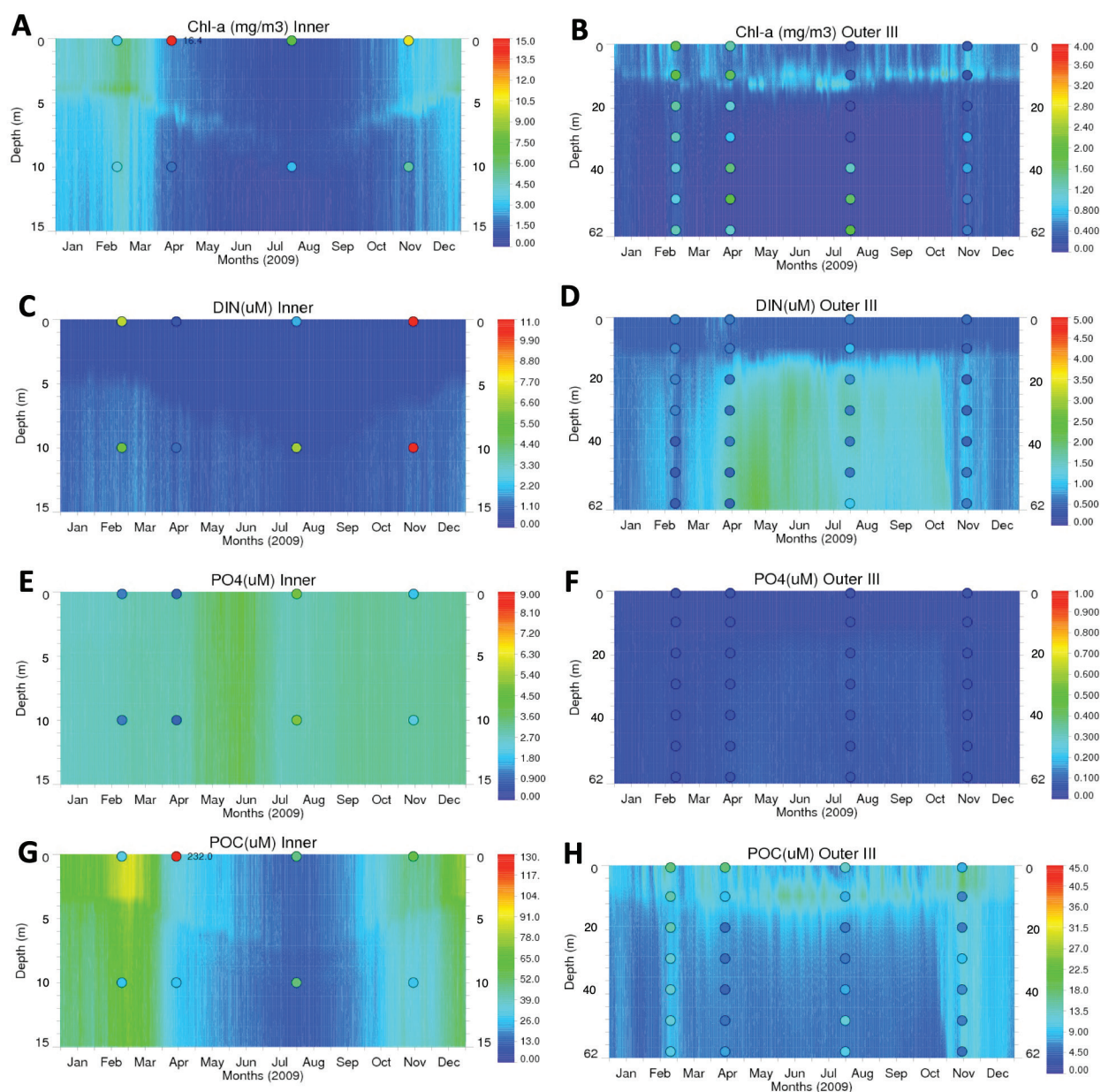
Medit. Mar. Sci., 22/3 2021, 677-696

687

Fig. 8: Time-depth distributions of simulation results (background) for 2009 in comparison to measurements (colored dots) of Chl-a (1st row), DIN (2nd row), PO4 (3rd row) and POC (last row) at the Inner Bay station (left column) and Outer Bay station (right column). Note the different scales used for Inner and Outer Bays.

weakness of the model is the absence of spring peaks in Chl-a due to the low levels of DIN which triggers lower production of fresh organic matter and therefore a lower POC concentration (being mainly phytoplankton in open sea waters, Sathyendranath *et al.,* 2009; Legendre & Michaud, 1999). The annual N/P ratio is much lower (0.5-6.0) than the classical Redfield ratio (16) (Redfield *et al.*, 1963), indicating N-limited algal production (Fig. 7). Although the model shows discrepancies with the field data (ave±sd: 4.7±4.2, Fig. 7), the main spatial and temporal distribution of the DIN/PO$_4$ ratio is depicted.

Time-depth distributions show a good representation of vertical distribution of Chl-*a* (Fig. 8A) in winter and autumn, but a weak performance for the rest of the year. Overall, measured DIN is higher than model results (Fig. 8C) for all depths and seasons with the exception of the month of April. PO$_4$ model results are vertically homoge-

neous in all seasons with no significant seasonal cycle, similar to observations (Fig. 8E). In winter and spring, model results are significantly higher than measured PO$_4$ at all depths, whereas there is a good agreement in summer and autumn. Vertical POC distribution (Fig. 8G) displays a similar seasonal cycle to Chl-*a*, higher in winter, minimum in summer and increasing in autumn and similarly shows higher observed surface POC concentrations than modelled in the Inner Bay in April (Fig. 8G). Both model and observations show minimal variation along the vertical profile.

Summarizing the model performance over the entire bay, the biogeochemical model results are more realistic when reproducing conditions in the Outer Bay, where a general oligotrophy driven by the influence of the Aegean Sea inflow is observed. A gradual decline in model performance was found towards Gediz River and inner

688

Medit. Mar. Sci., 22/3 2021, 677-696

regions, highly impacted by fresh water and external nutrient loads due to the anomalies in terrestrial inputs and their seasonal variations.

Ecosystem Model Validation

Ecosystem model validation revealed that the model represents the key biogeochemical features correctly. However, the ecosystem model does not perform as well as the hydrodynamic model, which was expected because of many non-linear interactions between model compartments.

Comparison of Chl-a model results with measurements over seasons and years (Table 3) shows model performance to be better in 2010 compared to 2009 in terms of both correlation and errors (Table 3). The best match occurs in winter seasons (Table 3). Misfit analysis of Chl-a suggests that model performance is better for lower values with underestimation of high Chl-a values (Fig. 9A). Errors increase towards shallower regions, with the largest mismatch located in the Inner Bay (statistics not shown).

The correlation between DIN model results and observations is mostly negative with relatively large errors (Table 3) indicating that the model could not accurately represent the highest concentrations. Error margins indicate best model performance for April with poorest fit in November. However, misfit analyses (Fig. 9B) reveal that the mismatch is not spatially homogeneous. The majority of DIN observations in Outer Bays (below 2 µM) are well represented by the model while modeled DIN values in the Inner and Middle Bays (above 2µM) are clearly underestimated (negative misfit). This is also confirmed by the low correlation and high RMSE and AAE values at high DIN values (data not shown).

Comparison of PO_4 model results with observations (Fig. 9C) shows that, except for some minimal mismatch, the model correlates well with measurements producing low statistical errors (Table 3). Misfit is relatively low in deeper regions and increases towards shallow areas (data not shown), signifying that model performance is better for oligotrophic environments compared to eutrophic conditions where the model slightly overestimates PO_4 concentrations.

Comparison between model results and POC measurements show good correlation but high errors, indicating that the general pattern of POC distribution is characterized, but with large bias in concentrations. Errors are minimal in deeper regions, especially in Outer III Bay, and increase towards shallower regions. Misfit analysis confirms that the model performs reasonably well at lower POC values (<40 µM) in the Outer Bays but fails to predict POC values in the Inner Bay (data not shown). In winter the model tends to overestimate, while in spring and summer it underestimates the observations.

Comparison with past data

In order to understand the ecosystem dynamics of Izmir Bay and the proficiency of the biogeochemical model simulation, model results and observations were compared with past data. Four main points from this comparison are discussed: i) extreme Chl-a and POC values in the Inner and Middle Bay; ii) characteristics of the

Table 3. Summary of statistics calculating model skill for chlorophyll a, DIN, PO4, and POC.

	Chlorophyll a (mg/m3)			DIN (µM)			PO$_4$ (µM)			POC (µM)		
	r	RMSE	AAE	r	RMSE	AAE	r	RMSE	AAE	R	RMSE	AAE
November 2008	0.24	2.27	1.97	0.13	7.65	2.59	0.98	0.20	0.09	0.35	28.30	8.83
February 2009	0.43	1.71	1.32	-0.07	2.17	0.96	0.93	0.58	0.22	0.68	18.10	9.52
April 2009	0.81	4.70	2.64	-0.31	0.76	0.61	0.86	0.56	0.19	0.69	27.70	23.80
July 2009	0.21	1.90	1.18	-0.26	1.24	0.68	0.99	0.56	0.22	0.61	18.80	9.20
November 2009	0.63	1.95	0.98	-0.11	3.77	1.63	0.71	0.67	0.30	0.61	10.90	7.15
February 2010	0.84	1.32	0.64	-0.06	2.01	1.18	0.88	1.02	0.41	0.80	23.60	15.40
April 2010	0.83	1.74	0.84	-0.21	0.96	0.61	0.89	0.55	0.20	0.84	9.05	7.58
July 2010	0.40	1.60	0.89	-0.3	1.25	0.96	0.93	0.46	0.21	0.57	12.50	8.97

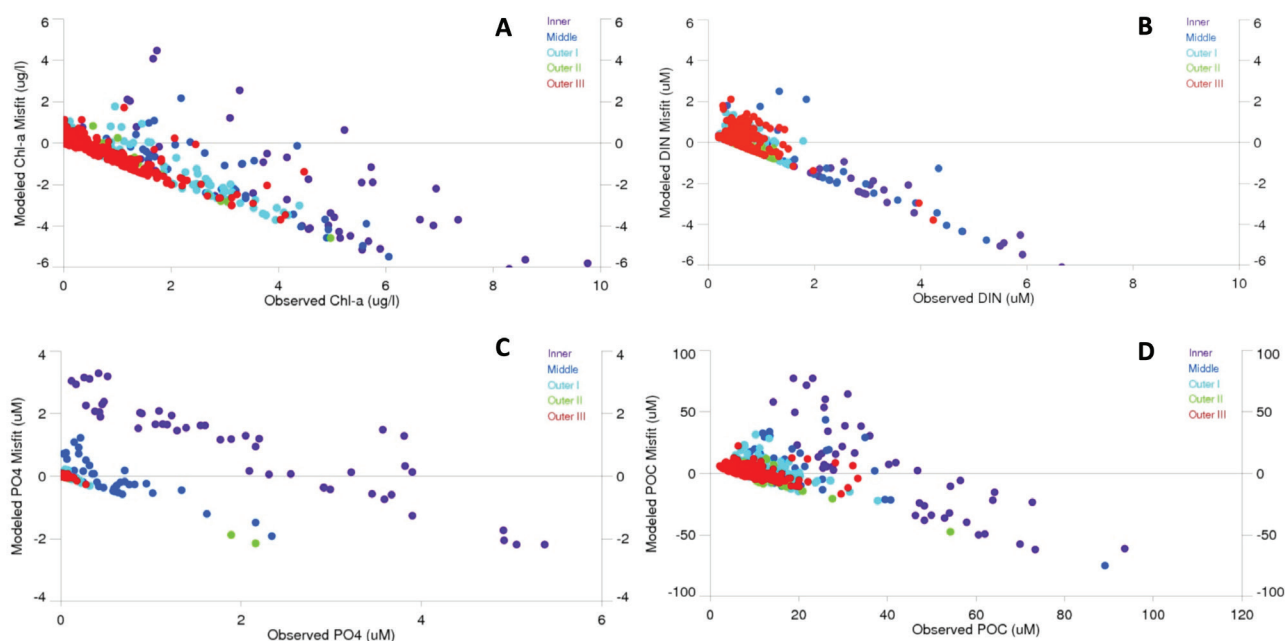*Medit. Mar. Sci.*, 22/3 2021, 677-696

689

Fig. 9: Measurements of model misfit (model-observations result) versus observations color coded with respect to region for A) Chl-a, B) DIN, C) PO4, and D) POC.

Gediz river area; iii) interactions between cyclonic-anticyclonic gyres and river inputs; iv) observed nutrient concentrations.

Chl-a distribution is reproduced with good spatial resolution over the entire study area. Discrepancies with observations occur mostly in areas where observed Chl-a is very high, and at depth where the deep chlorophyll maximum in the Outer Bay is not concurrent at the same depth with observations. Sensitivity tests carried out have shown that this mismatch is not related to the model representation of the seasonal thermocline fields, which indeed match observations well. More likely, the discrepancy has to be attributed to the light parameterization of the model.

Analogously, mismatches between observed and modeled POC are particularly evident in the most productive areas (Inner Bay). Some of these disparities can be attributed to the low DIN concentration simulated by the model which inhibits the start of the spring bloom. The low levels of modeled Chl-a may play a role in the low levels of POC, as phytoplankton is an important component of the total POC (Riley, 1971). Furthermore, analysis of the POC/Chl-a ratio in the observations (average ± st.dev.: 158 ± 132 w/w) indicates that the POC in Inner areas has a high content of detrital organic carbon, much above the value for living cells (range between 29 and 125 w/w according to phytoplankton type; Sathyendranath *et al.,* 2009; Graff *et al.,* 2015; Banse, 1977). This suggests that POC concentration is not only reflecting autochthonous primary production but instead should be associated to different processes like resuspension, and/or land-based inputs (Handa *et al.,* 2013; Riley, 1971). High POC concentrations (197 μM) were previously observed in the Inner-Middle Bay (Kucuksezgin *et al.,* 2005) and were associated, as in the present study, to a high POC/Chl-a ratio (450 w/w). In addition, Sunlu *et al.* (2011) reported that in some specific areas (Inner Bay: out of Melez and Middle Bay: out of

Cigli), POC concentrations in the sediments could not be attributed to the organic matter produced *in situ* and exported from the euphotic zone, but instead had to be related to external allochthonous loads. Based on these remarks, we hypothesize that the loads used to force the model may contain a depleted POC content, which might be an additional reason for the underestimation of modeled POC concentrations.

In the Gediz river area, the model simulates a DIN distribution with pronounced seasonal variability. Very high values of DIN occur in winter and spring triggering elevated chlorophyll and POC production. However, these extreme concentrations increase in an area markedly coastal and decrease sharply in offshore waters under the influence of the Aegean current. Unfortunately, the veracity of these peculiar features cannot be fully confirmed by the observations because the sampling stations (Fig. 1) do not include the river plume, but a station influenced by both Gediz river discharges and the Aegean current. Past observations in the estuarine waters (Bizsel *et al.,* 2017) showed a strong gradient in POC and Chl-a in proximity of the river mouth, with maximum values of POC (432 μM) and Chl-a, (8.51 mg m^{-3}) progressively decreasing towards the offshore waters. Interestingly, these data are in line with the values simulated by the model (POC: 120 μM; Chl-a: 15 mg m^{-3}) suggesting that the strong horizontal variation reported in the model reflects the variation of POC and Chl-a occurring in the area. The information available to simulate nutrients discharged by Gediz River are extremely fragmented, available only on a yearly basis and may be affected by bias. In addition, seasonal discharge data was not available, hence river fluxes used in the model are calculated based on the annual nutrient contents of the Gediz River (IMST-167, 2007; IMST-180, 2008) and monthly precipitation data, in an effort to reproduce a realistic seasonality in the River fluxes.

Field observations carried out during the two years of fieldwork show strong horizontal gradients of all biogeochemical parameters between the outer Bay and inner regions. Minimum and maximum values of nutrient concentrations were observed at the Outer and Inner Bay respectively, as previously described by many authors (Bizsel & Uslu, 2000; Bizsel *et al.*, 2009; Kucuksezgin, 2011; Sunlu *et al.*, 2012a,b, Aydin-Onen *et al.*, 2012; Kukrer & Buyukisik, 2013). This feature is caused by the presence of two sills at the entrance of the Inner and Outer bays (Fig. 1) which reduce water exchange with the innermost areas. In respect to previous observations carried out in 2001-2001 by Kucuksezgin *et al.* (2006), all areas display reductions in DIN and PO_4 concentrations (Table 4), while a significant Chlorophyll increase is reported for all regions and years.

Nutrient Enrichment versus Reduction Scenarios

The Delf3D modelling system was then used to test the impact of nutrient load changes on Izmir Bay with five different model simulations (see Table 1). The five model simulations carried out show a clear response in the biogeochemistry of the Bay, with specific regional peculiarities. Due to N-limited characteristics, Inner and Middle Bays are more responsive to changes in DIN where the increase/decrease in DIN input (runs A and B) resulted in a direct and proportional increase/decrease of primary production (Fig. 10). In contrast, variations in DIN inputs cause weak variations in the primary production of Outer Bays because of the P-limited properties, especially during winter and spring bloom periods. In particular, the weak decrease of Chl-a in response to DIN increase and conversely the weak increase of Chl-a in response to

Table 4. Field observations of DIN, PO4 and Chlorophyll a from this study (2008-2010) compared to previous observations undertaken before the Cigli WWTP was established.

|	Inner Bay	Change with respect to 2000-2001 (%)	Outer Bay	Change with respect to 2000-2001 (%)	Reference
2000-2001					
DIN (Ave ± St. Dev) (µM)	7.30±5.2		0.83±0.34		Kucuksezgin *et al.* (2006)
PO4 (µM)	1.50±1.10		0.08±0.07		Kucuksezgin *et al.* (2006)
Chl-a (mg m⁻³)	2.30±2.30		0.26±0.14		Kucuksezgin *et al.* (2006)
2008-2009					
DIN (µM)	5.04±1.15	-31	0.64±0.27	-23	current study
PO4 (µM)	1.45±1.50	-3	0.04±0.04	-50	current study
Chl-a (mg m⁻³)	4.86±4.59	111	1.58±1.09	508	current study
2009-2010					
DIN (µM)	3.09±3.42	-58	0.77±0.44	-7	current study
PO4 (µM)	1.06±1.89	-29	0.05±0.04	-38	current study
Chl-a (mg m⁻³)	3.97±3.05	73	0.63±0.56	142	current study
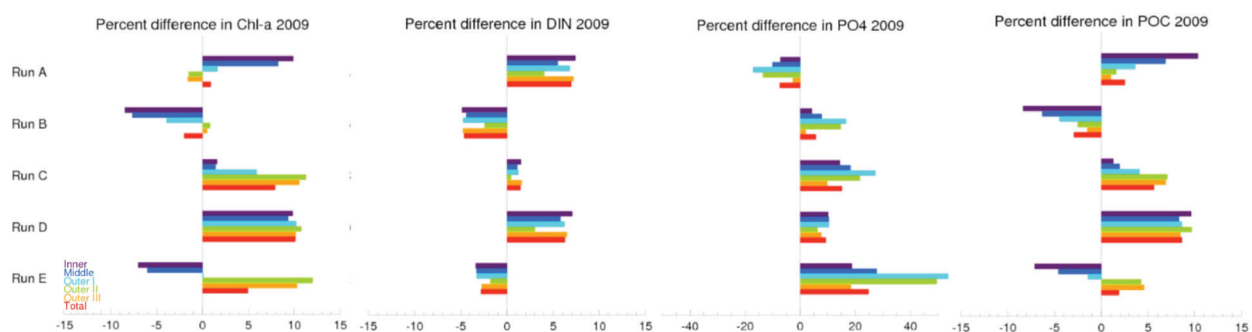
Fig. 10: Comparison of model ecosystem response of Izmir Bay to possible changes in nutrient loads in simulations A-E (see Table 1) for Chl-a, POC, DIN, and PO4. Results are given as percentage differences to the reference ecosystem run calculated as yearly averages for each of the sub-regions. Note the scale of percentage variation is 0-15% for all parameters with the exception of PO4 (0-50%).

Medit. Mar. Sci., 22/3 2021, 677-696

691

DIN decrease in the P-limited outer bays (Outer II and III) has to be attributed to the interconnection between the different areas of Izmir Bay. The increase of DIN input results in an increase of PO4 consumption in the Inner-Middle Bay and therefore a decrease of PO4 outflow to the P-limited Outer Bay. DIN inputs enhance N-limited primary production in Inner, Middle and Outer I Bays which are already characterized by high levels of PO_4. The opposite trend of PO_4 concentration to DIN increase/decrease is clearly explained by the limiting factors of primary production in each specific region. So, where N is the limiting factor, increased DIN loading drives consumption of PO_4 due to increased primary production. Conversely, reduction of DIN triggers an accumulation of PO_4 which cannot be consumed due to lack of N.

In run C (+10% PO_4), when only PO_4 is increased, primary production (Chl-a and POC) increases mainly in the P-depleted Outer Bay and to some extent in Middle Bay waters (Fig. 10). Escalated production in the Outer Bay is simply explained by P-limitation especially during the winter-spring period. However, the increase of production in the areas normally limited by nitrogen is more challenging to understand, as PO_4 is already in excess in these regions. The explanation comes from the changes in DIN levels. When adding PO_4 to the system, an increase of DIN levels is observed in all regions. Since a larger expanse of the Bay displays P-limitation (Outer Bays) rather than N-limitation (Inner and Middle Bays), the increase in PO_4 input boosts total production more than the increase in DIN input in previous simulations.

In run D (+10% PO_4 and +10% DIN), primary production (Chl-a and POC), DIN, and PO_4 concentrations increase in all regions simultaneously (Fig. 10). Indeed, the increase of DIN allows Inner and Middle Bays to be more productive, while the increase of PO_4 eliminates P-limitation in the Outer Bays.

In run E (+10% PO_4 and -10% DIN), the response of the Bay was again the sum of the responses given to individual changes in these nutrients (Fig. 10). Chl-a and POC decrease in Inner and Middle Bays which have low N/P ratios but increase in the P-limited Outer Bay waters with high N/P ratios.

Discussion

Circulation and physical properties of Izmir Bay

This study provides a detailed overview of seasonal variation in the physical properties of Izmir Bay, combining two years of physical observations (temperature and salinity) and model simulation results. This allowed for an extensive model validation that showed the model realistically reproduces the main features of the circulation.

Model simulations with the DELF3D model display several peculiar features of surface circulation in Izmir Bay: i) quasi-permanent cyclonic circulation in the outermost part of the Bay (Outer III), ii) anticyclonic circulation in the central regions (Outer I), and iii) anticyclonic circulation in the Inner Bay (Fig. 11). These main patterns are connected to the inflow of the Aegean Sea as well as the direction of the predominant winds in the Bay and their seasonal variability.

The simulated circulation in Outer III region is driven by the inflow of Aegean water at the northern boundary (Outer III) and forms a cyclonic circulation over much of the year (Fig. 11A). This reverses to an anticyclonic circulation only in the summer months (June to September) (Fig. 11B). Variability in this gyre in the Outer III region is observed, which agrees with previous studies (Ivanov *et al.*, 1998; Sayin, 2003; Sayin *et al.*, 2006). The current study finds Aegean Sea water entering mainly on the west and exiting along the east coast, however this pattern is reversed in summer, when Aegean Sea water enters from the east and exits close to the western coast as part of the reversal of the cyclonic circulation.

The CCMP wind forcing used in this study to force the circulation model shows strong north-westerly winds averaged for the month of February and particularly April, with predominantly weaker, more westerly winds in July (Supplementary Fig. S1). In summer, weak westerly winds prevail during August and September that increase to stronger westerly winds in November 2009 (Fig. S1). Ivanov *et al.* (1998) reported that the intensity of the currents is higher when westerly and northerly winds prevail, triggering a cyclonic circulation in the northern part of the Bay, while southerly and easterly
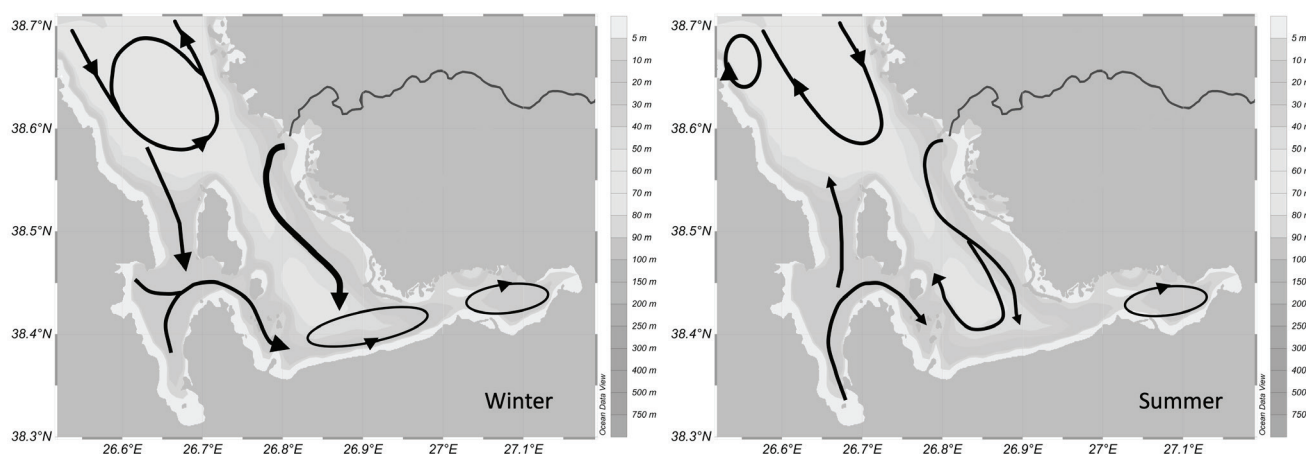

Fig. 11: General circulation of Izmir Bay in winter and summer as derived from model simulations.

692

Medit. Mar. Sci., 22/3 2021, 677-696

winds produce a weaker, anticyclonic circulation. Later, Sayin *et al.* (2006) found that southerly and easterly winds should limit the entrance of Aegean water, because of the northward directions of the surface currents. This hypothesis cannot be verified in our study, as during the 3 years of the simulation (2008-2010), the main wind direction did not change to southerly or easterly winds for a sufficiently long period of time. However, the wind direction during the summer months when the cyclonic circulation in the Outer Bay reverses in this study is north-westerly with frequent periods of calm indicating that the wind intensity may influence the circulation more than the direction.

The central region is characterized by a southward surface current (winter months) driven by the Gediz River outflow that provides water exchange with the Middle and Inner Bays. This feature evolves seasonally (summer) into a full anticyclonic gyre (Fig. 11B) which is associated with the anti-cyclonic circulation in Outer III region. In summer, the surface circulation is therefore dominated by a southward current carrying Aegean Sea inflow along the east coast with water from the river. The current flows along the east coast, which pushes the Aegean Sea water, enriched with the inputs of the Gediz River towards the Middle and Inner Bays. This anticyclonic gyre is mainly present during summer and early autumn, at a time of predominantly weak north-westerly winds. The same feature has been reported by Ivanov *et al.* (1998). Sayin *et al.* (2006) and Sayin & Eronat (2018) observed variability in this flow, reported as Middle gyre, dependent of the direction of the prevalent winds, with southerly winds causing a cyclonic circulation, which would prevent Aegean Sea surface water to further enter the Bay (Sayin *et al.*, 2006).

Furthermore, the Middle and Inner Bays are dominated by an anticyclonic circulation year-round, with water entering from the north coast and exiting in the south (Fig. 11). This feature has also been reported by Ivanov *et al.* (1998). However, the two additional modeling studies (Sayin, 2003; Sayin & Eronat, 2018) report a cyclonic circulation in the area. The water column in the inner regions is very well mixed in all seasons. This feature is confirmed by *in-situ* data, but was not reported by the other modeling studies. Most probably, the lower vertical resolution (6 sigma levels for Sayin's model and 8 z levels for Ivanov's model) hampered a good resolution of vertical dynamics in this area.

The current study included the influence of Aegean Sea water through an open boundary, which previous studies did not consider. Simulations show that Aegean Sea inflow is driving the circulation of the Outer Bay and influences circulation as far as the Middle Bay, while the circulation in the Outer Bay is less sensitive to wind. In the central regions of the Bay, weak wind conditions in summer are one factor facilitating the formation of the anticyclonic gyre in Outer I Bay. Additionally, the current study is the first to include fresh water inputs in a model of Izmir Bay. Simulation results show that freshwater inputs in both the Inner (small creeks, Çiğli WWTP outflow) and Outer Bay (Gediz River) have an impact on physical dynamics (Fig. 11) and a major influence on the biogeochemistry of the Bay (see section 4.2), in agreement with previous observations (Kucuksezgin *et al.*, 2006; Bizsel *et al.*, 2011). We emphasise here that the inflow of both Aegean Sea water and freshwater have transpired as major drivers of Izmir Bay circulation and be considered in future studies.

Biogeochemical properties of Izmir Bay

The biogeochemical model presented in this study is a significant step towards better understanding the nutrient dynamics of Izmir Bay. Owing to the coupling to a robust hydrodynamic model, the main biogeochemical dynamics connected to physical processes are correctly reproduced. Overall, spatial and seasonal distribution of biogeochemical parameters match the range of variation of the observations (Kucuksezgin *et al.*, 2006; Bizsel *et al.*, 2009; Sunlu *et al.*, 2012a,b), even though vertical gradients are not always well represented. The biogeochemical model has some difficulty generating extreme values occurring in coastal areas. As already discussed for the physical parameters, this mismatch is related to the high uncertainties in the terrestrial inputs used to force the model (very limited data available). On the other hand, the model is able to correctly describe the main nutrient limitation regime of the different areas, N-limitation in the Inner-Middle Bays and P-limitation in the Outer Bays (Kucuksezgin *et al.*, 2006; Bizsel *et al.*, 2009; Sunlu *et al.*, 2012b; Kukrer & Buyukisik, 2013). This suggests that the ecological and physico-biogeochemical dynamics and the balance between nutrient sources and sinks is well resolved.

Model simulations facilitate understanding of the interactions between river outflow and physical dynamics and the consequent nutrient fertilization effect on the Outer Bay. Depending on the season and physical dynamics, Gediz River plays a key role in the development of eutrophic conditions in the coastal waters outside of the river delta. Its influence is observed in the southern part of the Outer Bay (Outer I). Nutrient enriched surface water of the delta region is driven southward by an almost permanent coastal current during all seasons. Furthermore, the presence of a cyclonic gyre occurring north of Gediz inlet mainly in winter (Fig. 11 A) impacts the nutrient content of the coastal current. The southward current displays higher nutrient concentrations (Fig. 6), as it is mainly fed by Gediz River discharges. When an anticyclonic gyre occurs in summer (Fig. 11B), the coastal current is diluted by the oligotrophic Aegean Sea waters, which causes a decrease in nutrient concentration. Conversely, the presence of the cyclonic gyre blocks dilution by Aegean water inflow. This aspect needs to be taken into account when planning actions to prevent/mitigate eutrophication events in Outer I region.

The most important feature of the modeling approach used in this study is the inclusion of inflow from the Aegean Sea that affects nutrient circulation in the Bay. The inflow of low-nutrient water entering the northern area of

the Bay allows the generation of background levels of nutrients in the Outer Bays and at the same time dilutes the heavy nutrient loads discharged in the inner areas. This is also evident from the nutrient gradient observed from the Outer to the Inner Bays, correctly simulated for the first time by a biogeochemical model. To our knowledge, only two biogeochemical models have previously been developed for Izmir Bay (Buyukisik *et al.*, 1997; Sunlu *et al.*, 2011). However, as those models were very simplistic and did not include lateral advection, they lacked the capability to describe the spatial variability of Inner and Outer Bays. Moreover, the one-dimensional model of Buyukisik *et al.*, (1997) which was not able to detect the bloom periods.

The inclusion of river and urban discharges to the Bay in this model is a first attempt to resolve the influence of terrestrial inputs on the coastal and innermost areas and emerges as an important factor. This enables clarification of the main drivers influencing the innermost areas of the Bay in addition to the role of Gediz River for the productivity of the Outer Bay, which has been often described in the observations (Kontas *et al.,* 2004; Kucuksezgin, 2011). However, results should improve when a more detailed and complete dataset of input into the Bay becomes available.

A further important feature of the modeling approach in this study is the inclusion of the nutrient fluxes at the seawater-sediment interface. This enables the model account for the contribution of sediments to the water column nutrient concentration. However, the representation of the fluxes is quite simple. The Izmir area, in particular the Inner and Middle Bay, is characterized by sediments rich in organic and inorganic matter (Sunlu *et al.*, 2008; Aksu *et al.*, 1998) which is of consequence and should be considered and refined in future studies. Re-suspension events are reported to drive an intense flux of PO_4 and NH_4^+ from the sediment to the water column and the consumption of NO_3 in the sediments due to denitrification processes (Ozkan & Buyukisik, 2012; Ozkan *et al.*, 2008).

The ability of our model to reproduce the main nutrient limitation regime of the different regions is a key feature to understanding the spatial ecosystem response to future nutrient load scenarios. In particular, it illustrates that although future variations in nutrient loads to the Inner Bay will affect all areas of Izmir Bay, the responses to changes in DIN and PO_4 inputs will be radically different in the N-limited Inner Bays and the P-limited Outer Bays. In the context of possible mitigation actions, maintaining PO_4 inputs at the present level and decreasing DIN inputs (simulation B) would appear to be the best scenario among the solutions considered to reduce the eutrophication problem. The worst scenario, in terms of impact on the ecosystem's trophism would be an increase of both PO_4 and DIN inputs (simulation D) as this would trigger production in both the Inner and Outer Bays. In respect to the Inner Bay, which displayed the majority of eutrophication events in the past, the worst negative impact would be induced by an increase of the DIN fraction, independent of PO_4 inputs.

Conclusions

This 3D modeling study provides important progress in the knowledge of the ecosystem of Izmir Bay. Time-dependent circulation and biogeochemical dynamics of the entire Bay are described extensively for the first time. Model results were validated against observations showing a good representation of the physical and biogeochemical dynamics of the Bay, with less uncertainty for the physical parameters.

Model results demonstrate that the circulation in Izmir Bay is defined by the inflow of Aegean Sea water at the north of the Bay, a quasi-permanent cyclonic circulation in the outermost part of the Bay, and anticyclonic circulation in the central region, as well as in the Inner Bay. Thereby, the inflow of Aegean water, Gediz river inflow, as well as wind intensity play predominant roles over other factors in driving the circulation of the Bay.

Both physical and biogeochemical properties confirm a strong horizontal gradient due to high natural and anthropogenic nutrient inputs to the innermost areas. Local eutrophication conditions are reported in the proximity of direct wastewater discharges. The Gediz river area is heavily affected by nutrient loads which also marginally impact the Outer Bay. A key feature that emerged in this study is the different nutrient limitation regimes characterizing the Inner (N-limited) and Outer Bays (P-limited) as the reason for the contrasting ecosystem responses to DIN and PO_4 loads in different areas. According to the scenarios tested in this study, mitigation actions which aim to limit eutrophication events should reduce DIN inputs to the Inner Bays and PO_4 to the Outer Bay. Model uncertainty in the coastal and innermost areas can be reduced considerably reduced by means of better detailed description of terrestrial inputs.

Acknowledgements

References

Acara, A., Nalbantoglu, U., 1960. Preliminary report on the red tide outbreak in the Gulf of İzmir. *Rapports et procès-verbaux des réunions Commission internationale pour l'exploration scientifique de la Mer Méditerranée*, 5 (3), 3-38.

Aksu, A.E., Yasar, D., Uslu, O., 1998. Assessment of marine pollution in Izmir Bay: Heavy metal and organic compound

694

Medit. Mar. Sci., 22/3 2021, 677-696

concentrations in surficial sediments. *Turkish Journal of Engineering and Environmental Science*, 22, 387-415.

Aydin-Onen, S., Kocak, F., Kucuksezgin, F., 2012. Evaluation of spatial and temporal variations of inorganic nutrient species in the eastern Aegean Sea waters. *Marine Pollution Bulletin*, 64, 2849-2856.

Balk, D., Montgomery, M.R., McGranahan, G., Kim, D., Mara, V. *et al.,* 2009. Mapping urban settlements and the risks of climate change in Africa, Asia and South America. p. 80-103. In: *Population Dynamics and Climate Change.* Guzmán, J.M., Martine, G., McGranahan, G., Schensul, D., Tacoli, C., (Eds). United Nations Population Fund (UNFPA), International Institute for Environment and Development (IIED), New York.

Banse, K., 1977. Determining the carbon to chlorophyll ratio of natural phytoplankton. *Marine Biology*, 41, 199- 212.

Bizsel, N., Uslu, O., 2000. Phosphate, nitrogen and iron enrichment in the polluted Izmir Bay, Aegean Sea. *Marine Environmental Research*, 49 (2), 101-122.

Bizsel, N., Benli, H.A., Bizsel, C.K., Metin, G., 2001. A synoptic study on the phosphate and phytoplankton relationship in thehypereutrophicated Izmir Bay (Aegean Sea). *Turkish Journal of Engineering and Environmental Sciences*, 25, 89-99.

Bizsel, K.C., Ardelan, M.V., Bizsel, N., 2009. Iron budget and its correlations with macronutrients in the inshore waters of the Aegean Sea. *Estuaries and Coasts,* 32, 829-843.

Bizsel, K.C., Suzal, A., Demirdag, A., Inanan, B.E. Esen E., 2011. Particulate Organic Matter Contribution of Gediz River to the Aegean Sea. *Turkish Journal of Fisheries and Aquatic Sciences* 11, 547-559.

Bizsel, N., Ardelan, M.V., Bizsel, K. C., Suzal, A., Demirdag, A. *et al.,* 2017. Distribution of selenium in the plume of the Gediz River, Izmir Bay, Aegean Sea. *Journal of Marine Research,* 75 (2), 81-98.

Blauw, A.N., Los, H.F., Bokhorst, M., Erftemeijer, P.L., 2009. GEM: a generic ecological model for estuaries and coastal waters. *Hydrobiologia*, 618 (1), 175.

Buyukisik, B., Gokpinar, S., Parlak, H., 1997. Ecological modelling of İzmir Bay. *Journal of Fisheries and Aquatic Sciences,* 14 (1-2), 71-91.

Collet, I., Engelbert, A., 2013. Coastal regions. People living along the coastline, integration of NUTS 2010 and latest population grid. *Eurostat Statistics in focus*, 30, 212.

Delft Hydraulics, 2009. *Delft3D-FLOW User Manual.* Deltares, Delft, 684 pp. https://oss.deltares.nl/documents/183920/185723/Delft3D-FLOW_User_Manual.pdf

Gencay, H.A., Buyukisik, B., 2004. Effects of sewage outfall on phytoplankton community structure in Izmir Bay (Aegean Sea). *Ege University Journal of Fisheries and Aquatic Sciences*, 21, 107-111.

Graff, J.R., Westberry, T.K., Milligan, A.J., Brown, M.B., Dall'Olmo, G., 2015. Analytical phytoplankton carbon measurements spanning diverse ecosystems. *Deep Sea Research I* 102, 16-25.

Handa, N., Tanoue, E., Hama, T., 2013. *Dynamics and Characterization of Marine Organic. Matter*, Terra Scientific Publishing Company, Tokyo, 562 pp.

IMST, 1999. *Marine research in the Izmir Bay Project (1994-1998)*. Institute of Marine Science and Technology, Final report, Izmir.

IMST-167, 2007. *Monitoring of physical, chemical, biological and microbiological properties of Izmir Bay*. Technical Report. Institute of Marine Sciences and Technology, Izmir.

IMST-180, 2008. *Monitoring of physical, chemical, biological and microbiological properties of Izmir Bay*. Technical Report. Institute of Marine Sciences and Technology, Izmir.

Ivanov, V.A., Kubryakov, A.I., Mikhailova, E.N., Shapiro, N.B., 1997. Modelling of circulation in the Gulf of Izmir. *Physical Oceanography*, 8 (1), 47-55.

Ivanov, V.A., Kubryakov A.I., Shapiro, N.B., 1998. Thermohaline structure and dynamics of waters in the Izmir Bay. *Physical Oceanography*, 9 (4), 273-296.

Kocak, M., Kubilay, N., Tugrul, S., Mihalopoulos, N., 2010. Atmospheric nutrient inputs to the northern levantine basin from a long-term observation: sources and comparison with riverine inputs, *Biogeosciences,* 7, 4037-4050.

Kontas, A., Kucuksezgin, F., Altay, O., Uluturhan, E., 2004. Monitoring of eutrophication and nutrient limitation in the Izmir Bay (Turkey) before and after wastewater treatment plant. *Environment International* 29, 1057-1062.

Koray, T., Buyukisik, B., Parlak, H. Gokpinar, S., 1996. Eutrophication processes and algal blooms (red-tides) in İzmir Bay. *UNEP-MAP Technical Reports Series,* 104, 1-26.

Kucuksezgin, F., Kontas, A., Altay, O., Uluturhan, E., 2005. Elemental composition of particulate matter and nutrient dynamics in the Izmir Bay (Eastern Aegean). *Journal of Marine Systems,* 56 (1-2), 67-84.

Kucuksezgin, F., Kontas, A., Altay, O., Uluturhan, E., Darilmaz, E., 2006. Assessment of marine pollution in Izmir Bay: nutrient, heavy metal and total hydrocarbon concentrations. *Environment International,* 32, 41-51.

Kucuksezgin, F., 2011. The water quality of Izmir Bay: a case study. *Reviews of Environmental Contamination and Toxicology,* 211, 1-24.

Kukrer, S., Buyukisik, H.B., 2013. Size-fractionated phytoplankton and nutrient dynamics in the inner part of İzmir Bay, eastern Aegean Sea, *Turkish Journal of Botany,* 37, 177-187.

Legendre, L., Michaud, J., 1999. Chlorophyll a to estimate the particulate organic carbon available as food to large zooplankton in the euphotic zone of oceans. *Journal of Plankton Research,* 21, 2067-2083.

Lesser, G.R., Roelvink, J.A., van Kester, J.A.T.M., Stelling, G.S., 2004. Development and validation of a three-dimensional morphological model. *Journal of Coastal Engineering,* 51, 883-915.

Los, F.J., 2009. *Eco-hydrodynamic modelling of primary production in coastal waters and lakes using BLOOM (Vol. 1)*. IOS Press, Amsterdam.

Neumann, B., Vafeidis, A.T., Zimmermann, J., Nicholls, R.J., 2015. Future Coastal Population Growth and Exposure to Sea-Level Rise and Coastal Flooding - A Global Assessment. *PLoS ONE,* 10(3), e0118571.

Neumann, W., 1955. Fish mortalities event in Izmir Bay. *Hidrobiyoloji Mecmuasi,* A, 3 (2), 90-93.

Ozkan, E.Y., Kocatas, A., Buyukısık, B., 2008. Nutrient dynamics between sediment and overlying water in the inner part of Izmir Bay, Eastern Aegean. *Environmental Monitoring and Assessment,* 143, 313-325.

Medit. Mar. Sci., 22/3 2021, 677-696

695

Ozkan, E.Y., Buyukisik B., 2012. Examination of reactive phosphate fluxes in an eutrophicated coastal area. *Environmental Monitoring and Assessment*, 184, 3443-3454.

Redfield, A.C., Ketchum, B.H., Richards, F.A., 1963. The influence of organisms on the composition of sea-water. p. 26-77. In: *In the Sea, second edition.* Hill, N. (Ed.). Wiley, New York.

Riley, G.A., 1971. Particulate organic matter in sea water. *Advances in Marine Biology,* 8, 1-118.

Roelvink, J.A., van Banning, G.K.F.M., 1994. Design and Development of Delft-3D and application to coastal morphodynamics. p. 451-456. In: *Hydroinformatics '94.* Verwey, A., Minns, A.W., Babovic, V., Maksimovic, M. (Eds). Balkema, Rotterdam.

Sathyendranath, S., Stuart, V., Nair, A., Oka, K., Nakane, T. *et al*., 2009. Carbon-to-chlorophyll ratio and growth rate of phytoplankton in the sea. *Marine Ecology-Progress Series,* 383, 73-84.

Sayin, E., 2003. Physical features of the Izmir Bay. *Continental Shelf Research*, 23 (10), 957-970.

Sayin, E., Eronat, C., 2018. The dynamics of Izmir Bay under the effects of wind and thermohaline forces. *Ocean Sciences,* 14, 285-292.

Sayin, E., Pazi, I., Eronat, C., 2006. Investigation of water masses in Izmir Bay, western Turkey. *Turkish Journal of Earth Sciences,* 15, 343-372.

Small, C., Nicholls, R.J., 2003. A global analysis of human settlement in coastal zones. *Journal of Coastal Research*, 19, 584-599.

Stow, C.A., Jolliff, J., McGillicuddy, D.J., Doney, S.C., Allen, J. *et al.,* 2009. Skill assessment for coupled biological/physical models of marine systems. *Journal of Marine Systems,* 76 (1), 4-15.

Sunlu, U., Aydın, A., Egrihanci (Ozcetin), N.E., 2005. Investigation of carbon and organic matter (%) concentrations in the sediments of North Aegean Sea, (in Turkish), *E.U. Journal of Fisheries & Aquatic Sciences,* 22(3-4), 263-268.

Sunlu, U., Aksu, M., Buyukisik, B., Sunlu, F.S., 2008. Spatio-temporal variations of organic carbon and chlorophyll degradation products in the surficial sediments of Izmir Bay (Aegean Sea/Turkey). *Environmental Monitoring and Assessment,* 146 (1), 423-432.

Sunlu, F.S., Sunlu, U., Buyukisik, B., Kukrer, S., Aksu M., 2011. Effects of Wastewater Treatment Plant on Water Column and Sediment Quality in Izmir Bay (Eastearn Aegean Sea). p. 253-268. In: *Waste Water - Evaluation and Management*. García Einschlag, F.S. (Ed.). IntechOpen, Riyeka.

Sunlu, F.S., Sunlu, U., Buyukisik, B., Kukrer, S., Uncumusaoglu, A., 2012a. Nutrient and Chlorophyll a Trends after Wastewater Treatment Plant in Izmir Bay (Eastearn Aegean Sea). *Journal of Animal and Veterinary Advances,* 11, 113-123.

Sunlu, F.S., Sunlu, U., Buyukisik, B., Koray ,T., Kukrer, S. *et al.,* 2012b. The relationships between n:si:p molar ratio and coastal marine phytoplankton in Izmir Bay (Eastern Aegean sea–Turkey). *Fresenius Environmental Bulletin,* 21 (11b), 3376-3383.

TARAL-SINHA, 2011. *Urban Wastewater Management Along Coastal Areas of Turkey: Reidentification of Hot Spots and Sensitive Areas, Determination of Assimilation Capacities by Monitoring and Modelling and Development of Sustainable Urban Wastewater Investment Plans (TARAL-SINHA).* TUBITAK project, 107G066, final Technical Report.

UNEP/MAP, 1994. *Mediterranean Action Plan. Priority Actions Programme Regional Activity Centre (PAP/RAC). Integrated Management Study for the Area of Izmir*. MAP Technical Reports Series 84, 130 pp.

Yili Faaliyet Raporu, 2010. İzmir Su Ve Kanalizasyon İdaresi Genel Müdürlüğü. İzmir Büyük Belediyesi. https://www.izsu.gov.tr/tr/Dokumanlar/Liste/11

Yucel-Gier, G., Pazi, I., Kucuksezgin, F., Kocak, F., 2011. The composite trophic status index (TRIX) as a potential tool for regulation of Turkish marine aquaculture as applied to the eastern Aegean coast (Izmir Bay), *Applied Ichthyology,* 27, 39-45.

Supplementary data

The following supplementary information is available online for the article:
Fig. S1: Mean wind direction and speed over the greater Izmir Bay area from CCMP data used to force the model.

696

Medit. Mar. Sci., 22/3 2021, 677-696